

Gradient-Based Multi-Objective Deep Learning: Algorithms, Theories, Applications, and Beyond

Weiyu Chen*, Xiaoyuan Zhang*, Baijiong Lin*, Xi Lin, Han Zhao, Qingfu Zhang, *Fellow, IEEE*, and James T. Kwok, *Fellow, IEEE*

Abstract—Multi-objective optimization (MOO) in deep learning aims to simultaneously optimize multiple conflicting objectives, a challenge frequently encountered in areas like multi-task learning and multi-criteria learning. Recent advancements in gradient-based MOO methods have enabled the discovery of diverse types of solutions, ranging from a single balanced solution to finite or even infinite Pareto sets, tailored to user needs. These developments have broad applications across domains such as reinforcement learning, computer vision, recommendation systems, and large language models. This survey provides the first comprehensive review of gradient-based MOO in deep learning, covering algorithms, theories, and practical applications. By unifying various approaches and identifying critical challenges, it serves as a foundational resource for driving innovation in this evolving field. A comprehensive list of MOO algorithms in deep learning is available at <https://github.com/Baijiong-Lin/Awesome-Multi-Objective-Deep-Learning>.

Index Terms—Multi-Objective Optimization, Multi-Task Learning, Pareto Set Learning, Deep Learning

1 INTRODUCTION

Multi-Objective Optimization (MOO) [1], which aims to optimize multiple potentially conflicting objectives simultaneously, has become an important topic in deep learning. A multi-objective optimization problem can be formulated as:

$$\min_{\theta \in \mathcal{K} \subset \mathbb{R}^d} \mathbf{f}(\theta) := [f_1(\theta), \dots, f_m(\theta)]^T, \quad (1)$$

where $m \geq 2$ is the number of objectives, θ is the decision variable and $\mathcal{K} \subset \mathbb{R}^d$ is the feasible set of the decision variable.

Different from traditional single-objective optimization, which focuses on improving a single metric, MOO aims to obtain different solutions that achieve different trade-offs among objectives. Particularly, in MOO, users can specify their preferences regarding the relative importance of objectives, typically represented by a preference vector $\alpha = [\alpha_1, \dots, \alpha_m]^T \in \Delta_{m-1}$, where each α_i indicates the importance of the i -th objective and Δ_{m-1} denotes a $(m-1)$ -dimensional simplex. MOO is expected to achieve a solution that matches the user-defined preference. Hence, compared to single-objective optimization, MOO is more practical for complex real-world applications.

Originally arising from operations research, MOO has been extensively studied across various disciplines of science and engineering [2]. In recent years, there has been a surge of interest in applying MOO techniques to deep

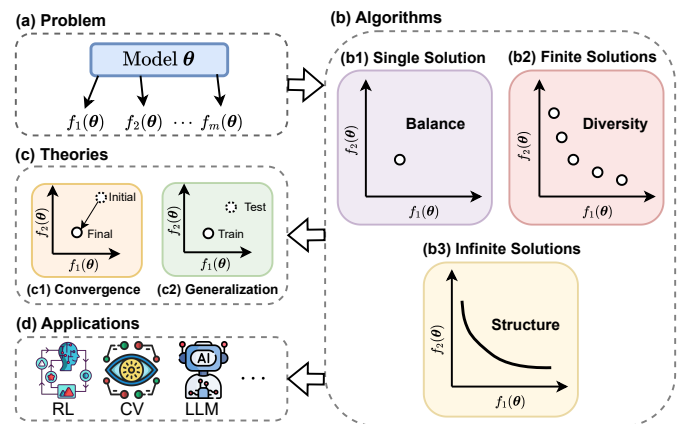


Fig. 1: An overview of multi-objective deep learning.

learning, leading to the reformulation or extension of many learning paradigms as MOO problems.

In deep learning, there are generally two primary types of MOO scenarios. One scenario is multi-task learning [3], where a model is trained to handle multiple tasks simultaneously. For example, in computer vision, we may desire a single network to perform various dense prediction tasks concurrently, such as segmentation, depth estimation, and surface normal prediction [4]. In reinforcement learning [5], we might aim for a model that performs well on several robotic manipulation tasks. In the training of Large Language Models (LLMs), we expect the model to excel at different tasks, such as mathematics, reasoning, language translation, and summarization. However, these tasks often compete for shared network resources, leading to conflicts that can degrade performance on individual tasks. By formulating the problem as an MOO, where the performance on each task is treated as a separate objective [6], we can systematically manage these conflicts and optimize all task

- The first three authors contributed equally.
- Weiyu Chen and James T. Kwok are with Department of Computer Science and Engineering, The Hong Kong University of Science and Technology. (E-mail: wchenbx@connect.ust.hk, jamesk@cse.ust.hk).
- Xiaoyuan Zhang, Xi Lin, and Qingfu Zhang are with Department of Computer Science, City University of Hong Kong. (E-mail: {xzhang2523-c, xi.lin}@my.cityu.edu.hk, qingfu.zhang@cityu.edu.hk).
- Baijiong Lin is with Artificial Intelligence Thrust, The Hong Kong University of Science and Technology (Guangzhou). (E-mail: bj.lin.email@gmail.com).
- Han Zhao is with Department of Computer Science, University of Illinois Urbana-Champaign. (E-mail: hanzhao@illinois.edu).
- Corresponding authors: Han Zhao, Qingfu Zhang, and James T. Kwok.

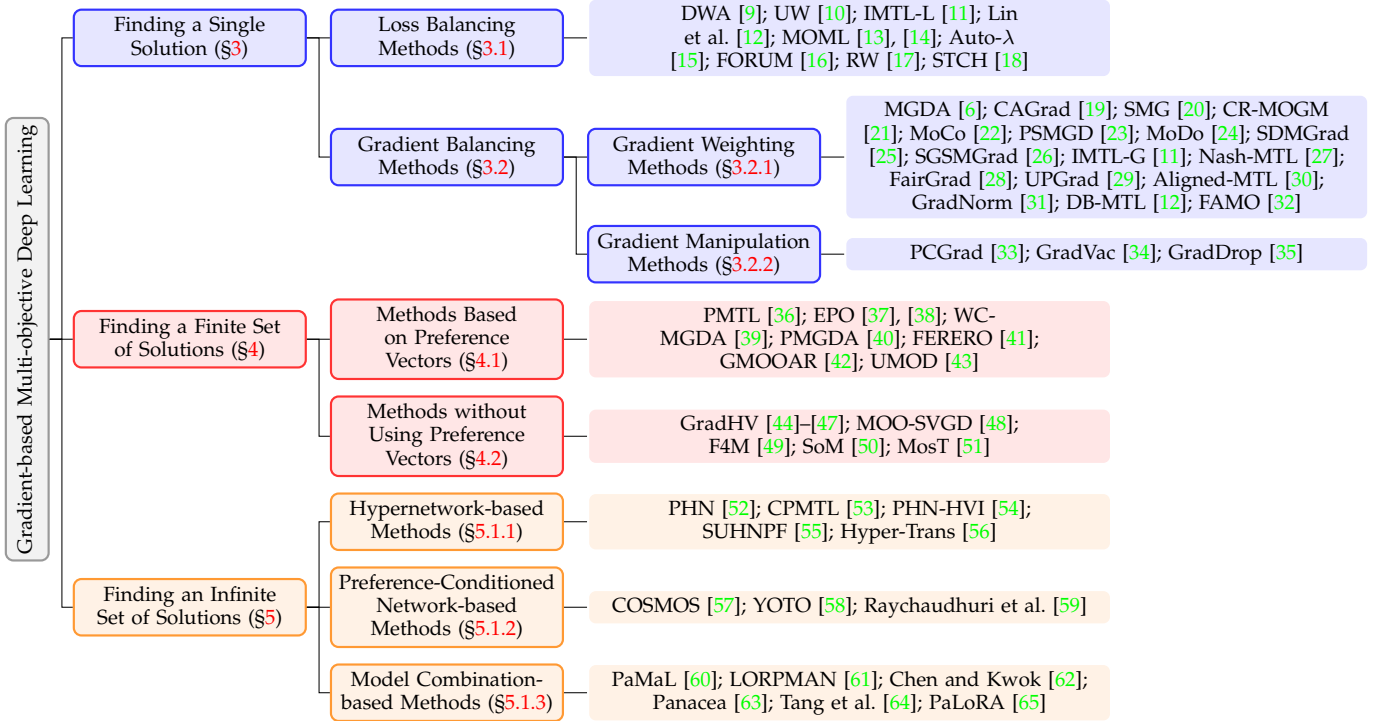


Fig. 2: Taxonomy of existing MOO algorithms in deep learning.

objectives simultaneously.

Another scenario involves incorporating additional evaluation criteria, such as fairness, safety, harmfulness mitigation, and efficiency, into learning paradigms. Considering these objectives is essential for practical real-world applications but may conflict with the primary goal of maximizing performance. For example, in LLMs training [7], we aim for models that not only perform well on tasks like language understanding but also adhere to safety standards, avoid producing harmful content, and ensure fairness across different users. In hardware-aware Neural Architecture Search (NAS) [8], we aim to discover network architectures that achieve high accuracy while also being efficient in terms of computational resources, energy consumption, or parameter size. However, reducing model size or computational complexity often leads to decreased performance. By treating such problems as MOO, where each criterion is an objective, we provide a structured way to explore these trade-offs.

1.1 Taxonomy

Instead of the traditional approach of directly summing all objectives into a single scalar function, MOO algorithms in deep learning can be categorized into three main approaches:

- To obtain a single, well-balanced solution, techniques like loss balancing and gradient balancing are employed to resolve conflicts between objectives during optimization. These methods focus on adjusting the weight of each objective to achieve a solution that is not overly biased toward any one objective.
- To obtain a finite set of Pareto optimal solutions, methods either divide the problem into subproblems using

preference vectors or directly optimize for multiple solutions simultaneously. This allows users to select from a set of solutions that best meet their specific needs.

- To generate an infinite set of Pareto optimal solutions, the focus shifts to learning a subspace of solutions rather than individual ones. Algorithms in this category propose efficient structures to learn this subspace. During training, preference vectors are randomly sampled in each iteration. Once a preference is sampled, the optimization reduces to solving for either a single solution or a finite set, making it possible to use techniques from the first two approaches.

Figure 2 illustrates the taxonomy of current MOO algorithms in deep learning, serving as a guide to the methods discussed in this paper. By exploring these avenues, MOO provides a comprehensive framework for addressing complex optimization problems in deep learning, enabling the development of models that can effectively balance multiple competing objectives.

1.2 Comparison with Related Surveys

Some surveys have attempted to cover aspects of MOO. For example, Zhang and Yang [3] provide a comprehensive overview of traditional multi-task methods within the machine learning domain. Crawshaw [66] offers a summary of multi-task methods in deep learning up to the year 2020. Yu et al. [67] present a comprehensive survey that covers multi-task learning from traditional machine learning to deep learning. Eichfelder [68] discusses advancements in MOO from a general optimization perspective, without specific emphasis on deep learning. Wei et al. [69] focus on evolutionary MOO algorithms, but these algorithms are usually not suitable for deep neural networks due to their large

TABLE 1: Summary of Notations.

Notation	Description
$\theta \in \mathcal{K} \subset \mathbb{R}^d$	Decision variable θ in feasible set \mathcal{K} with dimension d .
m	Number of objectives.
n	Number of finite Pareto solutions.
K	Number of iterations.
$f = [f_1, \dots, f_m]^\top$	Objective function.
$\lambda = [\lambda_1, \dots, \lambda_m]^\top$	Objective weight vector.
$\alpha = [\alpha_1, \dots, \alpha_m]^\top$	Preference vector.
$z^* = [z_1^*, \dots, z_m^*]^\top$	Ideal objective value.
$\theta^{(k)}$	Solution at k -th iteration.
$\theta^{(1)}, \dots, \theta^{(n)}$	Solution 1 to Solution n in a size- n solution set.
$g_i^{(k)}$	The gradient vector of i -th objective at k -th iteration.
$G^{(k)} = [g_1^{(k)}, \dots, g_m^{(k)}]$	Gradient matrix at k -th iteration.
$d^{(k)}$	Updating direction of θ at k -th iteration.
ϕ	Parameters of Pareto set learning structures.
$HV_r(\cdot)$	Hypervolume with respect to reference point r .
$[m]$	Index set $\{1, \dots, m\}$.
Δ_{m-1}	$(m-1)$ -D simplex $\{\alpha \mid \sum_{i=1}^m \alpha_i = 1, \alpha_i \geq 0, i \in [m]\}$.
$\ \cdot\ $	ℓ_2 norm.
η	Step size for updating θ .
ϵ	Error tolerance.

parameter spaces and computational demands. Peitz and Hoteigni [70] survey the MOO algorithms for deep learning but cover only a limited selection of gradient-based MOO methods and do not include theory and applications. Other surveys concentrate on applications of MOO in areas such as dense prediction tasks [4], recommend systems [71], and natural language processing [72].

Different with the previous surveys, this survey focuses on recent gradient-based MOO methods in deep learning, encompassing approaches for finding a single solution, a finite set of solutions, and an infinite set of solutions, and covering algorithms, theories, and applications. To the best of our knowledge, it is the first survey paper to focus on the gradient-based MOO methods in deep learning.

1.3 Organization of the Survey

The notations used in this survey are summarized in Table 1. An overview of MOO in deep learning is provided in Figure 1. The rest of this survey is organized as follows:

- Section 2 presents preliminaries in MOO, including key definitions and concepts;
- Section 3 discusses methods for finding a single Pareto optimal solution, covering loss balancing and gradient balancing approaches;
- Sections 4 and 5 focus on methods for identifying a finite and an infinite set of Pareto optimal solutions, respectively;
- Section 6 delves into the theoretical analysis of convergence and generalization in gradient-based multi-objective optimization algorithms;
- Section 7 showcases various applications in deep learning, including reinforcement learning, Bayesian optimization, computer vision, and large language models;
- Section 8 offers useful resources for multi-objective deep learning, such as datasets and software tools;
- Section 9 highlights challenges in the field and suggests promising directions for future research;
- Section 10 summarizes this survey.

2 PRELIMINARY: KEY CONCEPTS IN MOO

In this section, we first introduce some Pareto concepts in Section 2.1 and then review two classical methods (i.e.,

linear scalarization and Tchebycheff scalarization) to find Pareto solutions of MOO problems in defined in Section 2.2. An illustration of some Pareto concepts is in Appendix A.

2.1 Pareto Concepts

Unlike single-objective optimization, solutions in MOO cannot be directly compared based on a single criterion, but are compared using the concept of dominance as follows. Note that without loss of generality, we consider multi-objective minimization (i.e., problem (1)) here.

Definition 1 (strict) Pareto dominance [1]). A solution $\theta^{(a)}$ dominates another solution $\theta^{(b)}$ (denoted as $\theta^{(a)} \preceq \theta^{(b)}$) if and only if $f_i(\theta^{(a)}) \leq f_i(\theta^{(b)})$ for all $i \in [m]$, and there exists at least one $i \in [m]$ such that $f_i(\theta^{(a)}) < f_i(\theta^{(b)})$. A solution $\theta^{(a)}$ *strictly* dominates another solution $\theta^{(b)}$ if and only if $f_i(\theta^{(a)}) < f_i(\theta^{(b)})$ for all $i \in [m]$.

Based on this definition, we further define Pareto optimality (PO), Pareto set, and Pareto front as follows.

Definition 2 ((weak) Pareto optimality [1]). A solution θ^* is Pareto optimal if no other solution dominates it. A solution θ^* is *weakly* Pareto optimal if no other solution *strictly* dominates it.

Definition 3 (Pareto set (PS) and Pareto front (PF) [1]). A PS is the set of all PO solutions. A PF is the set of all objective function values of the PO solutions.

Definition 4 (Preference vector). α denotes a preference vector. The value of the entries of α denote the preference of a specific objective. Throughout this paper, a preference vector α is constrained on a simplex Δ_{m-1} , where $\Delta_{m-1} = \{\alpha \mid \sum_{i=1}^m \alpha_i = 1, \alpha_i \geq 0, i \in [m]\}$.

In deep learning, the parameter θ is typically optimized using gradient descent. In single-objective optimization, when the objective function is non-convex, the optimization process often reaches a stationary point. In the case of MOO, the solution generally converges to a *Pareto stationary* solution, which is defined as follows:

Definition 5 (Pareto stationary [73]). A solution θ^* is called *Pareto stationary* if there exists a vector $\lambda \in \Delta_{m-1}$ such that $\|\sum_{i=1}^m \lambda_i \nabla f_i(\theta^*)\| = 0$.

Pareto stationarity is a necessary condition for achieving Pareto optimality. If all objectives are convex with $\lambda_i > 0, \forall i$, it also serves as the Karush-Kuhn-Tucker (KKT) sufficient condition for Pareto optimality [73].

When evaluating the performance of a set of obtained solutions, the Hypervolume (HV) [74] indicator is one of the most widely used performance indicators, which is defined as follows.

Definition 6 (Hypervolume [74]). Given a solution set $\mathbb{S} = \{q^{(1)}, \dots, q^{(N)}\}$ and a reference point r , the hypervolume of \mathbb{S} is calculated by:

$$HV_r(\mathbb{S}) = \Lambda(\mathcal{P} \mid \exists q \in \mathbb{S} : q \preceq p \preceq r), \quad (2)$$

where $\Lambda(\cdot)$ denotes the Lebesgue measure of a set.

HV provides a unary measure of both convergence and diversity of a solution set. A larger HV indicates that the obtained solutions are diverse and their objective values are close to the PF.

2.2 Scalarization Methods

Linear scalarization. The most straightforward way to solve MOO problems is to reformulate them as single-objective optimization problems weighted by the given preference vector α as follows:

$$\min_{\theta \in \mathcal{K}} f_{\alpha}^{\text{LS}}(\theta) := \sum_{i=1}^m \alpha_i f_i(\theta). \quad (3)$$

Linear scalarization is widely used in practice due to its simplicity. However, this method suffers from a limitation: it can only identify solutions on the convex part of the PF. For PFs with a concave shape, using LS only finds the endpoints of a PF. **Tchebycheff scalarization.** Another way

to convert an MOP to a single one is to use the Tchebycheff scalarization function [75], [76], defined as:

$$\min_{\theta \in \mathcal{K}} f_{\alpha}^{\text{Tche}}(\theta) := \max_{i \in [m]} \alpha_i (f_i(\theta) - z_i^*), \quad (4)$$

where z_i^* are reference values, usually set as the ideal value of the i -th objective. Unlike linear scalarization, Tchebycheff scalarization can explore the entire PF by traversing all preference vectors within the simplex. This ensures that both convex and concave regions of the PF are covered. The relationship between Tchebycheff scalarization and weak Pareto optimality can be formally described as follows:

Theorem 1 ([77]). A solution θ^* of the original MOO problem (1) is weakly Pareto optimal if and only if there exists a preference vector α such that θ^* is an optimal solution of problem (4).

If θ^* is unique for a given α , it is considered Pareto optimal. However, Tchebycheff scalarization poses challenges for gradient-based deep learning due to the nonsmooth nature of the $\max(\cdot)$ operator. This nonsmoothness leads to non-differentiability and a slow convergence rate of $\mathcal{O}(1/\epsilon^2)$, where ϵ represents the error tolerance [18]. Even when all objectives $\{f_i\}_{i=1}^m$ are differentiable, problem (4) remains non-differentiable.

3 FINDING A SINGLE PARETO OPTIMAL SOLUTION

In some scenarios such as multi-task learning (MTL) [3], [66], [78], it is sufficient to identify a single Pareto optimal solution without the need to explore the entire Pareto set. Here, all objectives are usually treated as equally important (i.e., the preference vector is $\alpha = [\frac{1}{m}, \dots, \frac{1}{m}]^T$), and the goal is to produce a single model that effectively balances all objectives. The most straightforward method is the linear scalarization method (i.e., problem (3)) with $\alpha_i = \frac{1}{m}$, which is known as Equal Weighting (EW) [3] in MTL. However, EW may cause some tasks to have unsatisfactory performance [12], [79]. Therefore, to improve the performance, many methods have been proposed to dynamically tune the objective weights $\{\lambda_i\}_{i=1}^m$ during training, which can in general be formulated as:

$$\min_{\theta} \sum_{i=1}^m \lambda_i f_i(\theta), \quad (5)$$

where λ_i is the weight for the i -th objective $f_i(\theta)$ and the uniform preference vector α is omitted for simplicity. These

methods can be categorized as loss balancing methods and gradient balancing approaches. Some representative loss/gradient balancing methods are illustrated in Figure 3 (adapted from [11], [19]).

3.1 Loss Balancing Methods

This type of approach dynamically computes or learns the objective weights $\{\lambda_i\}_{i=1}^m$ during training using some measures on loss such as the decrease speed of loss [9], homeostatic uncertainty of loss [10], loss scale [11], [12], and validation loss [13]–[16].

Dynamic Weight Average (DWA) [9] estimates each objective weight as the ratio of the training losses in the last two iterations. Formally, the objective weight in k -th iteration ($k > 2$) is computed as follows:

$$\lambda_i^{(k)} = \frac{m \exp(\omega_i^{(k-1)}/\gamma)}{\sum_{j=1}^m \exp(\omega_j^{(k-1)}/\gamma)}, \quad \omega_j^{(k-1)} = \frac{f_j^{(k-1)}}{f_j^{(k-2)}}, \quad (6)$$

where γ is the temperature and $f_i^{(k)}$ is the loss value of i -th objective at k -th iteration.

Kendall et al. [10] propose Uncertainty Weighting (UW) that considers the homoscedastic uncertainty of each objective and optimizes objective weights together with the model parameter as follows:

$$\min_{\theta, \mathbf{s}} \sum_{i=1}^m \left(\frac{1}{2s_i^2} f_i(\theta) + \log s_i \right), \quad (7)$$

where $\mathbf{s} = [s_1, \dots, s_m]^T$ is learnable and $\log s_i$'s are regularization terms.

Impartial Multi-Task Learning (IMTL) [11] balances losses across tasks, abbreviated as IMTL-L(oss). Specifically, IMTL-L encourages all objectives to have a similar loss scale by transforming each objective $f_i(\theta)$ as $e^{s_i} f_i(\theta) - s_i$. Similar to UW [10], IMTL-L simultaneously learns the transformation parameter \mathbf{s} and the model parameter θ as follows:

$$\min_{\theta, \mathbf{s}} \sum_{i=1}^m (e^{s_i} f_i(\theta) - s_i). \quad (8)$$

Similar to IMTL-L [11], Lin et al. [12] also aim to make all objective losses have a similar scale. They achieve it by performing a logarithm transformation on each objective (i.e., $\log f_i(\theta)$). Moreover, they theoretically show that the transformation in IMTL-L is equivalent to the logarithm transformation when s_i is the exact minimizer of $\min_{s_i} e^{s_i} f_i(\theta) - s_i$ in each iteration. Hence, the logarithm transformation can recover the transformation in IMTL-L.

Ye et al. [13], [14] propose Multi-Objective Meta Learning (MOML), which adaptively tunes the objective weights λ based on the validation performance, reformulating problem (5) as a multi-objective bi-level optimization problem:

$$\min_{\lambda} [f_1(\theta^*(\lambda); \mathcal{D}_1^{\text{val}}), \dots, f_m(\theta^*(\lambda); \mathcal{D}_m^{\text{val}})]^T \quad (9a)$$

$$\text{s.t. } \theta^*(\lambda) = \arg \min_{\theta} \sum_{i=1}^m \lambda_i f_i(\theta; \mathcal{D}_i^{\text{tr}}), \quad (9b)$$

where $\mathcal{D}_i^{\text{tr}}$ and $\mathcal{D}_i^{\text{val}}$ are the training and validation datasets for the i -th objective, respectively. In each training iteration, when given objective weights $\{\lambda_i\}_{i=1}^m$, MOML first learns

the model $\theta^*(\lambda)$ on the training dataset by solving lower-level (LL) subproblem (9b) with T iterations and then updates λ in the upper-level (UL) subproblem (9a) via minimizing the loss of the trained MTL model $\theta^*(\lambda)$ on the validation dataset of each objective. However, when solving the UL subproblem (9a), MOML needs to calculate the complex hypergradient $\nabla_{\lambda}\theta^*(\lambda)$ which requires to compute many Hessian-vector products via the chain rule. Hence, the time and memory costs of MOML grow significantly fast with respect to the dimension of θ and the number of LL iterations T .

Auto- λ [15] modifies problem (9) by replacing the multi-objective UL subproblem (9a) with a single-objective problem: $\min_{\lambda} \sum_{i=1}^m f_i(\theta^*(\lambda); \mathcal{D}_i^{\text{val}})$. Besides, Auto- λ approximates the hypergradient $\nabla_{\lambda}\theta^*(\lambda)$ via the finite difference approach. Thus, it is more efficient than MOML [13], [14].

Recently, FORUM [16] is proposed to improve the efficiency of MOML [13], [14]. FORUM first reformulates problem (9) as a constrained MOO problem via the value-function approach [80] and then proposes a multi-gradient aggregation method to solve it. Compared with MOML, FORUM is a first-order method and does not need to compute the hypergradient $\nabla_{\lambda}\theta^*(\lambda)$. Thus, it is significantly more efficient than MOML.

Random Weighting (RW) [17] randomly samples objective weights from a distribution (such as the standard normal distribution) and normalizes them into the simplex in each iteration. Compared to EW, RW has a higher probability of escaping local minima than EW due to the randomness from objective weights, resulting in better generalization performance.

Different from the above methods which are based on linear scalarization, Lin et al. [18] propose Smooth Tchebycheff scalarization (STCH), which transforms the Tchebycheff scalarization into a smooth function:

$$\min_{\theta} f_{\alpha}^{\text{STCH}}(\theta, \mu) := \mu \log \sum_{i=1}^m \exp(\alpha_i(f_i(\theta) - z_i^*)/\mu), \quad (10)$$

where $\mu > 0$ is a smoothing parameter, and z^* is a reference point as in Tchebycheff scalarization (problem (4)). STCH improves upon the original Tchebycheff scalarization by making $f_{\alpha}^{\text{STCH}}(\theta, \mu)$ smooth when all objective functions $f_i(\theta)$'s are smooth, resulting in faster convergence. It also retains the advantages of the original Tchebycheff scalarization: (1) convexity when all objective functions are convex and (2) Pareto optimality by appropriately choosing μ .

3.2 Gradient Balancing Methods

Let $\mathbf{g}_i^{(k)} = \nabla_{\theta} f_i(\theta)|_{\theta^{(k)}} \in \mathbb{R}^d$ be the gradient of the i -th objective at the k -th iteration. This type of approach aims to find a common update direction $\mathbf{d}^{(k)}$ by adaptively aggregating the gradients of all objectives $\{\mathbf{g}_i^{(k)}\}_{i=1}^m$ at each iteration. Then, the model parameter is updated via $\theta^{(k+1)} = \theta^{(k)} - \eta \mathbf{d}^{(k)}$, where η is a step size. To simplify notations, we omit the superscript in this section. Compared with loss balancing methods in Section 3.1, the gradient balancing approach usually achieves better performance.

3.2.1 Gradient Weighting Methods

In most gradient weighting methods, \mathbf{d} is computed by:

$$\mathbf{d} = \mathbf{G}\boldsymbol{\lambda}, \quad (11)$$

where $\mathbf{G} = [\mathbf{g}_1, \dots, \mathbf{g}_m] \in \mathbb{R}^{d \times m}$ is the gradient matrix and $\boldsymbol{\lambda} = [\lambda_1, \dots, \lambda_m]^{\top}$ is the gradient weights.

Sener and Koltun [6] apply Multiple-Gradient Descent Algorithm (MGDA) [73], which aims to find a direction \mathbf{d} at each iteration to maximize the minimal decrease across the losses. This is formulated as:

$$\max_{\mathbf{d}} \min_{i \in [m]} (f_i(\theta) - f_i(\theta - \eta \mathbf{d})) \approx \max_{\mathbf{d}} \min_{i \in [m]} \mathbf{g}_i^{\top} \mathbf{d}, \quad (12)$$

where η is the step size. The solution of problem (12) is $\mathbf{d} = \mathbf{G}\boldsymbol{\lambda}$, where $\boldsymbol{\lambda}$ is computed as:

$$\boldsymbol{\lambda} = \arg \min_{\boldsymbol{\lambda} \in \Delta_{m-1}} \|\mathbf{G}\boldsymbol{\lambda}\|^2, \quad (13)$$

where Δ_{m-1} denotes the simplex. Sener and Koltun [6] use the Frank-Wolfe algorithm [81] to solve problem (13).

Conflict-Averse Gradient descent (CAGrad) [19] improves MGDA [6] by constraining the aggregated gradient \mathbf{d} to be around the average gradient $\mathbf{g}_0 = \frac{1}{m} \sum_{i=1}^m \mathbf{g}_i$ with a distance $c \|\mathbf{g}_0\|$, where $c \in [0, 1]$ is a constant. Specifically, \mathbf{d} is computed by solving the following problem:

$$\max_{\mathbf{d}} \min_{i \in [m]} \mathbf{g}_i^{\top} \mathbf{d}, \quad \text{s.t. } \|\mathbf{d} - \mathbf{g}_0\| \leq c \|\mathbf{g}_0\|. \quad (14)$$

Problem (14) is equivalent to first computing $\boldsymbol{\lambda}$ by solving the following problem:

$$\boldsymbol{\lambda} = \arg \min_{\boldsymbol{\lambda} \in \Delta_{m-1}} \mathbf{g}_{\boldsymbol{\lambda}}^{\top} \mathbf{g}_0 + \|\mathbf{g}_0\| \|\mathbf{g}_{\boldsymbol{\lambda}}\|, \quad (15)$$

where $\mathbf{g}_{\boldsymbol{\lambda}} = \frac{1}{m} \mathbf{G}\boldsymbol{\lambda}$ and then calculate the update direction $\mathbf{d} = \mathbf{g}_0 + \frac{c}{\|\mathbf{g}_{\boldsymbol{\lambda}}\|} \mathbf{g}_{\boldsymbol{\lambda}}$. Note that CAGrad is simplified to EW when $c = 0$ and degenerates into MGDA [6] when $c \rightarrow +\infty$.

MGDA [6] and its variant CAGrad [19] can converge to a Pareto stationary point in the deterministic setting with full-gradient computations. However, in deep learning, where stochastic gradients are used, many works [20]–[26] explore the convergence properties of MGDA under stochastic gradients, which are introduced in detail in Section 6.1.

IMTL-G(rad) [11] aims to find \mathbf{d} that has equal projections on all objective gradients. Thus, we have:

$$\mathbf{u}_1^{\top} \mathbf{d} = \mathbf{u}_i^{\top} \mathbf{d}, \quad 2 \leq i \leq m, \quad (16)$$

where $\mathbf{u}_i = \mathbf{g}_i / \|\mathbf{g}_i\|$. If constraining $\sum_{i=1}^m \lambda_i = 1$, problem (16) has a closed-form solution of $\boldsymbol{\lambda}$:

$$\boldsymbol{\lambda}_{(2, \dots, m)} = \mathbf{g}_1^{\top} \mathbf{U} (\mathbf{D}\mathbf{U}^{\top})^{-1}, \quad \lambda_1 = 1 - \sum_{i=2}^m \lambda_i, \quad (17)$$

where $\boldsymbol{\lambda}_{(2, \dots, m)} = [\lambda_2, \dots, \lambda_m]^{\top}$, $\mathbf{U} = [\mathbf{u}_1 - \mathbf{u}_2, \dots, \mathbf{u}_1 - \mathbf{u}_m]$, and $\mathbf{D} = [\mathbf{g}_1 - \mathbf{g}_2, \dots, \mathbf{g}_1 - \mathbf{g}_m]$.

Nash-MTL [27] formulates problem (11) as a bargaining game [82], [83], where each objective is cast as a player and the utility function for each player is defined as $\mathbf{g}_i^{\top} \mathbf{d}$. Hence, \mathbf{d} is computed by solving the following problem:

$$\max_{\mathbf{d}} \sum_{i=1}^m \log(\mathbf{g}_i^{\top} \mathbf{d}). \quad (18)$$

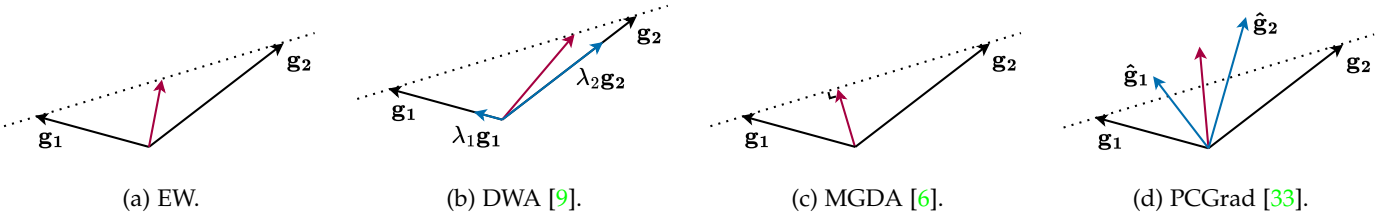


Fig. 3: Illustration of the update direction d of several representative methods: EW, DWA [9] from loss balancing methods, MGDA [6] from gradient weighting methods, and PCGrad [33] from gradient manipulation methods. They are illustrated in a two-objective learning problem (two specific gradients are labeled as g_1 and g_2).

The solution of problem (18) is $d = G\lambda$, where λ is obtained by solving the following problem:

$$G^T G \lambda = \lambda^{-1}, \quad (19)$$

which can be approximately solved using a sequence of convex optimization problems.

FairGrad [28] extends Nash-MTL [27] by computing λ through the equation $G^T G \lambda = \lambda^{-1/\gamma}$, where $\gamma \geq 0$ is a constant. Unlike Nash-MTL [27], FairGrad treats the problem as a constrained nonlinear least squares problem. Similarly, UPGrad [29] calculates λ by optimizing $\min_{\lambda} \lambda^T G^T G \lambda$, a quadratic programming (QP) problem.

Aligned-MTL [30] considers problem (11) as a linear system and aims to enhance its stability by minimizing the condition number of G . Specifically, the Gram matrix $C = G^T G$ is first computed. Then, the eigenvalues $\{\sigma_1, \dots, \sigma_R\}$ and eigenvectors V of C are obtained. Finally, λ is computed by:

$$\lambda = \sqrt{\sigma_R} V \Sigma^{-1} V^T, \quad (20)$$

where $\Sigma^{-1} = \text{diag}(\sqrt{1/\sigma_1}, \dots, \sqrt{1/\sigma_R})$.

Gradient Normalization (GradNorm) [31] aims to learn λ so that the scaled gradients have similar magnitudes. It updates λ by solving the following problem via one-step gradient descent:

$$\min_{\lambda} \sum_{i=1}^m (\|\lambda_i g_i\| - c \times r_i^\gamma), \quad (21)$$

where $c = \frac{1}{m} \sum_{i=1}^m \|\lambda_i g_i\|$ is the average scaled gradient norm and is treated as a constant, $r_i = \frac{f_i/f_i^{(0)}}{\frac{1}{m} \sum_{j=1}^m (f_j/f_j^{(0)})}$ is the training speed of the i -th objective and is also considered as a constant, and $\gamma > 0$ is a hyperparameter.

Dual-Balancing Multi-Task Learning (DB-MTL) [12] also normalizes all objective gradients to the same magnitude. λ is computed as $\lambda_i = \gamma/\|g_i\|$, where $\gamma = \max_{i \in [m]} \|g_i\|$ is a scaling factor controlling the update magnitude. Thus, compared with GradNorm [31], this method guarantees all objective gradients have the same norm in each iteration. Moreover, they observe that the choice of the update magnitude γ significantly affects performance.

3.2.2 Gradient Manipulation Methods

To address the conflicting gradient problem, gradient manipulation methods correct each objective gradient g_i to \hat{g}_i and then compute the update direction as $d = \sum_{i=1}^m \hat{g}_i$.

Projecting Conflicting Gradients (PCGrad) [33] considers two objective gradients g_i and g_j as conflicting if $g_i^T g_j < 0$. Then, it corrects each objective gradient by projecting it onto the normal plane of other objectives' gradients. Specifically, at each iteration, \hat{g}_i is initialized with its original gradient g_i . Then, for each $j \neq i$, if $\hat{g}_i^T g_j < 0$, \hat{g}_i is corrected as:

$$\hat{g}_i = \hat{g}_i - \frac{\hat{g}_i^T g_j}{\|g_j\|^2} g_j. \quad (22)$$

This reduces gradient conflicts by removing the components of \hat{g}_i that oppose other objective gradients.

While PCGrad [33] corrects the gradient if and only if two objectives have a negative gradient similarity, Gradient Vaccine (GradVac) [34] extends it to a more general and adaptive formulation. In each iteration, if $\phi_{ij} < \bar{\phi}_{ij}$, GradVac updates the corrected gradient \hat{g}_i as:

$$\hat{g}_i = \hat{g}_i - \frac{\|\hat{g}_i\| (\bar{\phi}_{ij} \sqrt{1 - \phi_{ij}^2} - \phi_{ij} \sqrt{1 - \bar{\phi}_{ij}^2})}{\|g_j\| \sqrt{1 - \bar{\phi}_{ij}^2}} g_j, \quad (23)$$

where ϕ_{ij} is the cosine similarity between \hat{g}_i and g_j . $\bar{\phi}_{ij}$ is initialized to 0 and updated by Exponential Moving Average (EMA), i.e., $\bar{\phi}_{ij} \leftarrow (1 - \beta)\bar{\phi}_{ij} + \beta\phi_{ij}$, where β is a hyperparameter. Note that GradVac simplifies to PCGrad when $\bar{\phi}_{ij} = 0$.

Gradient Sign Dropout (GradDrop) [35] considers that conflicts arise from differences in the sign of gradient values. Thus, a probabilistic masking procedure is proposed to preserve gradients with consistent signs during each update.

3.2.3 Practical Speedup Strategy

Gradient balancing methods suffer from high computational and storage costs. Specifically, in each iteration, almost all gradient balancing methods require performing m back-propagation processes to obtain all objective gradients w.r.t. the model parameter $\theta \in \mathbb{R}^d$ and then store these gradients $G \in \mathbb{R}^{d \times m}$. This can be computationally expensive when dealing with a large number of objectives or using a neural network with a large number of parameters. Moreover, many gradient balancing methods (such as MGDA [6], CAGrad [19], Nash-MTL [27], and FairGrad [28]) need to solve an optimization problem to obtain the objective weight λ in each iteration, which also increases the computational and memory costs. Hence, several strategies are proposed to alleviate this problem.

Sener and Koltun [6] use feature-level gradients (i.e., gradients w.r.t. the representations from the last shared

layer) to replace the parameter-level gradients (i.e., gradients w.r.t. the shared parameters θ). Since the dimension of the representation is much smaller than that of the shared parameters, it can significantly reduce the computational and memory costs. This strategy is also adopted by some gradient balancing methods, such as IMTL-G [11] and Aligned-MTL [30].

Liu et al. [19] randomly select a subset of objectives to calculate the update direction in each iteration. Navon et al. [27] propose to update the objective weight λ every τ iterations instead of updating in each iteration. Although this strategy speeds up training, they observe that it may cause a noticeable drop in performance. Liu et al. [32] consider optimizing the logarithm of the MGDA objective [6] and propose a speedup strategy. Specifically, when solving problem (13) via one-step gradient descent, λ is updated as $\lambda \leftarrow \lambda - \eta \nabla_{\lambda} \|\mathbf{G}\lambda\|^2$. Note that

$$\begin{aligned} \frac{1}{2} \nabla_{\lambda} \|\mathbf{G}\lambda\|^2 &= \mathbf{G}^{\top} \mathbf{G}\lambda = \mathbf{G}^{\top} \mathbf{d} \\ &\approx \frac{1}{\eta} \left[f_1^{(k)} - f_1^{(k+1)}, \dots, f_m^{(k)} - f_m^{(k+1)} \right]^{\top}, \end{aligned} \quad (24)$$

where $f_i^{(k)}$ is the loss value of the i -th objective in the k -th iteration. Hence, λ can be approximately updated using the change in losses without computing all objective gradients. Although this strategy significantly reduces computational and memory costs, it may cause performance degradation. Moreover, it is only applicable to MGDA-based methods.

3.3 Discussions

Loss balancing and gradient balancing methods effectively mitigate conflicts among different objectives and achieve a Pareto-optimal solution, which is important for MOO scenarios such as multi-task learning. However, they are limited to finding a single Pareto-optimal solution and lack the ability to control the solution's position on the Pareto front, resulting in inapplicability in some scenarios such as multi-criteria learning. In Sections 4 and 5, we introduce methods to achieve more diverse and controllable solutions.

The computational cost of loss balancing methods (except MOML [13], [14], Auto- λ [15], and FORUM [16]) is almost the same as that of EW since they only need one backpropagation process in each training iteration. However, gradient balancing methods are much more computationally expensive due to the need of m backpropagation processes to obtain each objective gradient, where m is the number of objectives. Although some speedup strategies are proposed to alleviate this problem, they may cause a drop in performance, as detailed in Section 3.2.3. Compared to loss balancing methods, gradient balancing methods generally exhibit better convergence properties such as guaranteeing to converge to a Pareto stationary point, as detailed in Section 6.1.

4 FINDING A FINITE SET OF SOLUTIONS

In some scenarios, a single solution may be insufficient to balance the objectives, as users may prefer to obtain multiple trade-off solutions and select one based on their specific needs. This section introduces algorithms to identify a finite

set of solutions, providing a discrete approximation of the Pareto set. We first discuss methods based on preference vectors (Section 4.1), followed by approaches that do not require the use of preference vectors (Section 4.2). Solutions obtained by some representative methods on LSMOP1 [84] are shown in Figure 4, with additional details and more results provided in Appendix B.

4.1 Methods Based on Preference Vectors

Preference vector-based methods rely on a preference vector set $\{\alpha^{(1)}, \dots, \alpha^{(n)}\}$. These preference vectors partition the problem into n subproblems, where each subproblem involves finding the solution that corresponds to a specific preference vector in the set. By solving n subproblems, these methods obtain a set of n solutions.

Pareto Multi-Task Learning (PMTL) [36], inspired by the idea of decomposition-based MOO algorithms [85], incorporates preference vectors as constraints on the objectives. For the i -th subproblem with preference vector $\alpha^{(i)}$, the objective vector $\mathbf{f}(\theta)$ is constrained to be closer to $\alpha^{(i)}$ than to the other preference vectors:

$$\begin{aligned} \min_{\theta \in \mathcal{K} \subset \mathbb{R}^d} \mathbf{f}(\theta) &:= [f_1(\theta), \dots, f_m(\theta)]^{\top}, \\ \text{s.t. } r^{(j)}(\theta) &:= (\alpha^{(j)} - \alpha^{(i)})^{\top} \mathbf{f}(\theta) \leq 0, \quad j \in [n]. \end{aligned} \quad (25)$$

Let \mathbf{R} be the matrix containing gradients of the active constraints, i.e. $\mathbf{R} = [\nabla r^{(j)}(\theta)]_{j \in \mathbb{I}(\theta)}$, with $\mathbb{I}(\theta) = \{j \in [n] \mid r^{(j)}(\theta) \geq -\epsilon\}$ containing indices of the active constraints. Using a method akin to MGDA [6], PMTL derives a descent direction for problem (25) that optimizes all m objectives while keeping $\mathbf{f}(\theta)$ within the sector closer to the preference vector $\alpha^{(i)}$. The descent direction is:

$$\mathbf{d} = -\mathbf{G}\lambda + \mathbf{R}\beta, \quad (26)$$

where $\mathbf{G} = [\nabla f_1(\theta), \dots, \nabla f_m(\theta)]$ is the gradient matrix. λ and β are coefficients obtained by solving:

$$\begin{aligned} \lambda, \beta &= \arg \min_{\lambda, \beta} \|\mathbf{G}\lambda + \mathbf{R}\beta\|^2, \\ \text{s.t. } \lambda^{\top} \mathbf{1} + \beta^{\top} \mathbf{1} &= 1, \quad \lambda_i \geq 0, \quad \beta_j \geq 0. \end{aligned} \quad (27)$$

A limitation of PMTL is its weak constraint that only requires the objective vector to lie within sectors, which lacks precise control over the position of Pareto solutions.

Exact Pareto Optimal search (EPO) [37], [38] is designed to locate Pareto solutions which are aligned the objective vector exactly with given preference vectors. EPO achieves this using a uniformity function, $u_{\alpha}(\mathbf{f}(\theta)) = \text{KL}(\hat{\mathbf{f}}(\theta) \parallel \mathbf{1}/m)$, where: $\hat{f}_i(\theta) = \frac{\alpha_i f_i(\theta)}{\sum_{j=1}^m \alpha_j f_j(\theta)}$. Minimizing this function aligns $\mathbf{f}(\theta)$ with α , achieving precise alignment and Pareto optimality. Let $\mathbf{C} = \mathbf{G}^{\top} \mathbf{G}$ and \mathbf{c}_i be the i -th column of \mathbf{C} . Let $\mathbf{a} = [a_1, \dots, a_m]^{\top}$, where $a_i = \alpha_i (\log(m \hat{f}_i(\theta)) - u_{\alpha}(\mathbf{f}(\theta)))$. At each iteration, EPO classifies objective indices into three sets: $\mathbb{J} = \{j \mid \mathbf{a}^{\top} \mathbf{c}_j > 0\}$ are the indices decreasing uniformity, $\bar{\mathbb{J}} = \{j \mid \mathbf{a}^{\top} \mathbf{c}_j \leq 0\}$ are the indices increasing uniformity, and \mathbb{J}^* are the indices with the max-

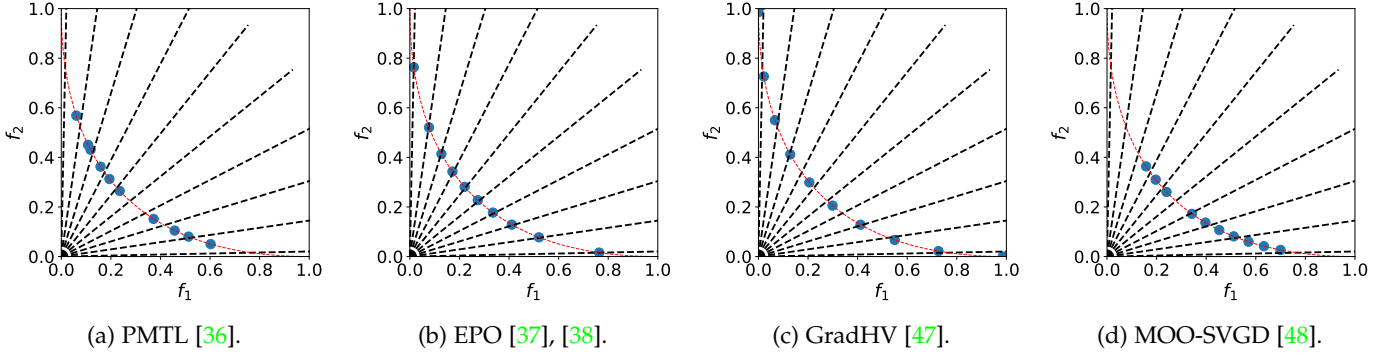


Fig. 4: Distributions of solutions obtained by using representative methods: PTML [36] and EPO [37], [38] are preference vector-based methods, while GradHV [47] and MOO-SVGD [48] are methods not using preference vectors. The blue circles denote the solutions, the red curves denote the ground truth PF and the black lines denote the preference vectors.

imum $\alpha_j f_j(\boldsymbol{\theta})$. Based on these sets, it determines $\boldsymbol{\lambda}$ for the common descent direction $\mathbf{d} = \mathbf{G}\boldsymbol{\lambda}$ by solving:

$$\begin{aligned} \boldsymbol{\lambda} &= \arg \max_{\boldsymbol{\lambda} \in \Delta_{m-1}} \boldsymbol{\lambda}^\top \mathbf{C}(\mathbf{a}\mathbb{1}_{u_\alpha} + \mathbf{1}(1 - \mathbb{1}_{u_\alpha})), \\ \text{s.t. } &\begin{cases} \boldsymbol{\lambda}^\top \mathbf{c}_j \geq \mathbf{a}^\top \mathbf{c}_j \mathbb{1}_J, & \forall j \in \bar{J} \setminus J^*, \\ \boldsymbol{\lambda}^\top \mathbf{c}_j \geq 0, & \forall j \in J^*. \end{cases} \end{aligned} \quad (28)$$

This updating direction can balance objectives while reducing non-uniformity, resulting in solutions that exactly match each preference vector. However, EPO has three drawbacks: (1) objective vectors must be non-negative, (2) unnecessary complexity from dividing sets into three subsets, and (3) computational inefficiency due to repeated Jacobian calculations and solving linear programming problem (i.e., problem (28)).

To address these limitations, Weighted Chebyshev MGDA (WC-MGDA) [39] considers the dual form of Tchebycheff scalarization (problem (4)) of a linear programming problem. Optimizing Tchebycheff function addresses the previously mentioned drawbacks of EPO. However, its convergence rate is relatively slow. Two concurrent approaches have been proposed to improve the Tchebycheff scalarization: (1) smooth Tchebycheff scalarization (problem (10)) [18] that smooths the original non-smooth max operation, and (2) the Preference-based MGDA (PMGDA) [40] that requires only a negative inner product of the updating direction with the "exact" constraint gradient.

FERERO [41] captures preference information within the MGDA framework, addressing both objective constraints with constants and the exactness constraint. It achieves fast convergence rates of $\mathcal{O}(\epsilon^{-1})$ for deterministic gradients and $\mathcal{O}(\epsilon^{-2})$ for stochastic gradients, where ϵ is the error tolerance.

The methods discussed above rely on a fixed set of preference vectors. However, in real-world applications where the shape of the Pareto front is unknown, a predefined set of preference vectors may not always result in well-distributed solutions. To overcome this limitation, GMOOAR [42] formulates the problem as a bi-level optimization problem. In the upper level, preference vectors are optimized to maximize either the hypervolume or uniformity of the solutions. In the lower level, solutions are optimized based on these preference vectors. This approach enables the algorithm to dynamically adjust preference vectors based on the given

optimization problem, ensuring the desired solution distribution. UMOD [43] introduces an approach that aims to maximize the minimum distance between solutions:

$$\max \min_{1 \leq i < j \leq n} \rho(\mathbf{f}(\boldsymbol{\theta}^{(i)}), \mathbf{f}(\boldsymbol{\theta}^{(j)})), \text{ s.t. } \boldsymbol{\theta}^{(i)}, \boldsymbol{\theta}^{(j)} \in \text{PS}, \quad (29)$$

where $\rho(\cdot, \cdot)$ denotes the Euclidean distance. UMOD achieves desirable solution distributions with theoretical guarantees: (1) For bi-objective problems with a connected, compact PF, the optimal solution includes the PF endpoints, with equal distances between neighboring objective vectors; (2) As the number of solutions increases, the objective vectors asymptotically distribute on the PF.

4.2 Methods without Using Preference Vectors

Another line of research, directly optimize for a diverse set of Pareto-optimal solutions, does not rely on a given set of preference vectors.

As HV evaluates solution sets based on both convergence and diversity, it is commonly used in traditional evolutionary MOO [86]. In the context of gradient-based MOO, gradient-based hypervolume maximization algorithms (GradHV) [44]–[47] have been developed. Let $\{\boldsymbol{\theta}^{(1)}, \dots, \boldsymbol{\theta}^{(n)}\}$ be a set of solutions and $\{\mathbf{f}(\boldsymbol{\theta}^{(1)}), \dots, \mathbf{f}(\boldsymbol{\theta}^{(n)})\}$ be their corresponding objective vectors. These algorithm first calculate the hypervolume gradient of the i -th solution $\boldsymbol{\theta}^{(i)}$ as follows:

$$\mathbf{d}^{(i)} = \sum_{k=1}^m \underbrace{\frac{\partial \text{HV}_r(\{\mathbf{f}(\boldsymbol{\theta}^{(1)}), \dots, \mathbf{f}(\boldsymbol{\theta}^{(n)})\})}{\partial f_k(\boldsymbol{\theta}^{(i)})}}_{\mathbf{a}_i: 1 \times 1} \underbrace{\frac{\partial f_k(\boldsymbol{\theta}^{(i)})}{\partial \boldsymbol{\theta}^{(i)}}}_{\mathbf{B}: 1 \times d}. \quad (30)$$

Once $\mathbf{d}^{(i)}$ is calculated, solutions $\boldsymbol{\theta}^{(i)}$'s are updated by gradient ascent, $\boldsymbol{\theta}^{(i)} \leftarrow \boldsymbol{\theta}^{(i)} + \eta \mathbf{d}^{(i)}$, where η is a learning rate. The term \mathbf{B} in Equation (30) can be easily estimated via backpropagation. The main challenge lies in estimating the first term \mathbf{a}_i . Following Emmerich et al. [46], index sets are categorized based on differentiability: \mathbb{Z} includes subvectors with zero partial gradients, \mathbb{U} contains subvectors with undefined or indeterminate gradients, and \mathbb{P} has subvectors with positive gradients. This classification leads to many zero-gradient terms, improving efficiency. Then, non-zero terms are computed using a fast dimension-sweeping algorithm [87], [88]. This method applies to bi-, tri-, and four-objective problems with time complexities

of $\Theta(mn + n \log n)$ for $m = 2$ or 3 and $\Theta(mn + n^2)$ for $m = 4$, where m is the number of objectives and n is the number of solutions. To further enhance convergence, the Newton-hypervolume method [89] incorporates second-order information for faster updates. Deist et al. [44] apply the hypervolume gradient methods for deep learning tasks such as medical image classification with more than thousands of parameters.

Inspired by Stein Variational Gradient Descent (SVGD) [90], MOO-SVGD [48] proposes a different approach to maintain diversity while enhancing convergence. The update direction for the i -th solution $\theta^{(i)}$ is given by:

$$\begin{aligned} \mathbf{d}^{(i)} = & - \sum_{j=1}^n \mathbf{g}^*(\theta^{(j)}) \kappa(\mathbf{f}(\theta^{(i)}), \mathbf{f}(\theta^{(j)})) \\ & + \mu \nabla_{\theta^{(i)}} \kappa(\mathbf{f}(\theta^{(i)}), \mathbf{f}(\theta^{(j)})). \end{aligned} \quad (31)$$

where $\mathbf{g}^*(\theta^{(j)}) = \sum_{i=1}^m \lambda_i^* \nabla f_i(\theta^{(j)})$, and $\{\lambda_i^*\}_{i=1}^m$ are the objective weights obtained by MGDA [6] (i.e., problem (13)). $\kappa(\cdot, \cdot)$ represents a kernel function, often chosen as the radial basis function (RBF) kernel. The first term in (31) guides the solution towards the PS, while the second term pushes the solutions away from each other to enhance the diversity.

The methods discussed above focus on scenarios where the number of solutions n exceeds the number of objectives m . Recent works [49]–[51], [91] explore the case with more objectives than solutions (i.e., $m > n$). These approaches assign each objective to a solution $\theta \in \{\theta^1, \dots, \theta^n\}$ that achieves the smallest objective value for that particular objective. They then minimize either the maximum or the sum of these smallest objective values. Few for Many (F4M) [49], [91] uses the maximum aggregation, formulated as:

$$\min_{\theta^1, \dots, \theta^n} \max_{i \in [m]} \min_{\theta \in \{\theta^1, \dots, \theta^n\}} f_i(\theta). \quad (32)$$

Sum of Minimum (SoM) [50] uses the sum aggregation, formulated as:

$$\min_{\theta^1, \dots, \theta^n} \sum_{i=1}^m \left(\min_{\theta \in \{\theta^1, \dots, \theta^n\}} f_i(\theta) \right). \quad (33)$$

MosT [51] frames the problem as a bilevel optimization task, with the outer loop using MGDA to optimize solutions and the inner loop solving an optimal transport problem to assign objectives to solutions.

4.3 Discussions

This section reviews two primary approaches for obtaining multiple Pareto optimal solutions.

Preference vector-based methods decompose an MOO problem into multiple independent subproblems based on predefined preference vectors. These subproblems can be solved independently, which enhances memory efficiency and enables parallel computation. However, in real-world applications, determining suitable preference vectors can be challenging due to the complex and often unpredictable nature of the Pareto front. Furthermore, since the subproblems are solved independently, they cannot benefit from shared information between one another.

On the other hand, methods not using preference vectors bypass the challenge of selecting preference vectors by

directly optimizing a set of solutions. These methods generate a set of Pareto-optimal solutions that inherently share interdependent information. However, this approach typically requires higher memory resources and incurs greater computational costs, making it less efficient in resource-constrained scenarios.

5 FINDING AN INFINITE SET OF SOLUTIONS

While a finite set of solutions can only provide a discrete approximation of the Pareto front, many applications require the ability to obtain solutions corresponding to any user preference, effectively representing the entire Pareto set. Directly learning an infinite number of solutions individually is impractical.

Ma et al. [92] initially investigated deriving an infinite set of solutions by approximating the Pareto set with first-order expansion around discrete Pareto-optimal solutions. However, this method has several drawbacks: (1) The approximation error grows when the solutions are widely spaced, (2) First-order approximations perform poorly in high-dimensional objective spaces, and (3) The approach requires solving a linear programming problem for updates, which can be computationally challenging.

To address these issues, many methods have been introduced that leverage neural networks to learn mappings from user preferences to solutions directly, enabling the capture of the entire PS. These methods rely on designing efficient network architectures and implementing effective training strategies.

In Section 5.1, we introduce various network structures designed to capture the entire PS through preference-based mappings. Specifically, current algorithms mainly use three types of network structures: (1) Hypernetwork in Section 5.1.1, (2) Preference-Conditioned Network in Section 5.1.2, and (3) Model Combination in Section 5.1.3. An illustration of these methods is shown in Figure 5. Section 5.2 discusses training strategies for these network structures.

5.1 Network Structure

5.1.1 Hypernetwork

Hypernetwork is a neural network that generates the parameters for another target network [93]. This idea has been leveraged by the Pareto Hypernetwork (PHN) [52] and Controllable Pareto Multi-Task Learning (CPMTL) [53] to learn the entire Pareto set, where the input is the user preference α and the output is the target network’s parameters. The hypernetwork usually consists of several MLP layers, and has been adopted in many subsequent approaches such as PHN-HVI [54] and SUHNPf [55]. Recently, Tuan et al. [56] propose using a transformer architecture as the hypernetwork, which demonstrates superior performance compared to MLP-based hypernetwork models.

A primary limitation of hypernetwork-based algorithms is their sizes. Since the output dimension matches the number of parameters in the target network, hypernetworks are often much larger than the base networks, limiting their applicability to large models. Some methods address this limitation by employing hypernetworks with chunking [52], [53]. Chunking involves partitioning the parameter

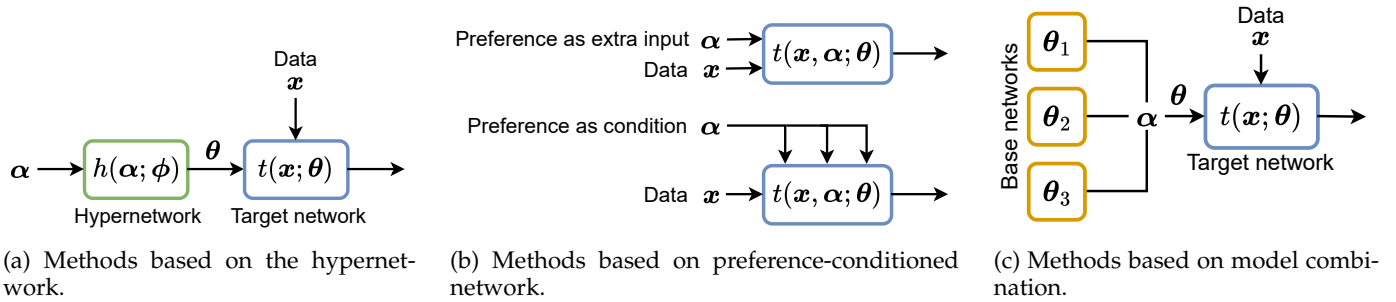


Fig. 5: Illustration of different structures to learn an infinite number of solutions.

space into smaller, more manageable segments, enabling the hypernetwork to generate parameters more efficiently and scalability. This approach reduces the overall size of the hypernetwork while preserving its capability to produce accurate parameters for the target network.

5.1.2 Preference-Conditioned Network

Instead of using a hypernetwork to generate weights, the original model can be directly modified to incorporate preferences. COSMOS [57] suggests adding preferences as an additional input to the model by combining user preference α with input data x , thereby increasing the input dimension of the original neural network.

However, such input-based conditioning has limited ability to produce diverse solutions. Some studies [42], [58], [59] employ the Feature-wise Linear Modulation (FiLM) layer [94] to condition the network. The FiLM layer works by applying an affine transformation to the feature maps. Specifically, given a feature map u with C channels, we use an MLP to generate conditioning parameters $\gamma \in \mathbb{R}^C$ and $\beta \in \mathbb{R}^C$ based on the given preference α . Then, the FiLM layer modifies the features as $u'_c = \gamma_c \cdot u_c + \beta_c$, where u_c is the c -th channel of u . This method achieves better conditioning ability compared to merely adding the preference to the input layer. Raychaudhuri et al. [59] also propose leveraging another network to predict the network architecture. It dynamically adapts the model's structure according to user preferences, allowing for more flexible and efficient learning.

5.1.3 Model Combination

Methods based on model combination construct a composite model by integrating multiple individual models, thereby offering an effective way to introduce diversity. PaMaL [60] achieves this by learning several base models and combining them through a weighted sum of their parameters based on user preferences:

$$\theta(\alpha) = \sum_{i=1}^m \alpha_i \theta_i. \quad (34)$$

Although this incorporates more parameters than methods based on preference-conditioned networks, PaMaL enhances diversity and provides users with a broader range of choices.

Despite its benefits, learning multiple models simultaneously may become inefficient when handling a large number of objectives. To mitigate this issue, LORPMAN [61]

proposes learning a full-rank model $\theta_0 \in \mathbb{R}^{p \times q}$ and m low-rank models $B_i A_i$'s, where $B_i \in \mathbb{R}^{p \times r}$ and $A_i \in \mathbb{R}^{r \times q}$. Given user preference α , the composite model is given by:

$$\theta(\alpha) = \theta_0 + s \sum_{i=1}^m \alpha_i B_i A_i, \quad (35)$$

where s is a scaling factor that adjusts the impact of the low-rank components. This approach efficiently scales Pareto set learning to manage up to 40 objectives, achieving superior performance. A similar approach is also mentioned in [65]. To further enhance parameter efficiency, Chen and Kwok [62] introduce a preference-aware tensor multiplication:

$$\theta(\alpha) = \theta_0 + s C \times_1 A \times_2 B \times_3 \alpha, \quad (36)$$

where $C \in \mathbb{R}^{r \times r \times m}$ is a learnable core tensor, $A \in \mathbb{R}^{r \times p}$, $B \in \mathbb{R}^{r \times q}$ are learnable matrices, and \times_u denotes mode- u tensor multiplication [95]. Zhong et al. [63] address scalability challenges for large-scale models, such as language models, using SVD:

$$\theta(\alpha) = \theta_0 + U \Sigma V, \quad (37)$$

where $U \in \mathbb{R}^{p \times (r+m)}$ and $V \in \mathbb{R}^{(r+m) \times q}$ are learnable matrices. Σ is a diagonal matrix defined as $\text{diag}(\sigma_1, \dots, \sigma_r, s\alpha_1, \dots, s\alpha_m)$, where $\{\sigma_i\}_{i=1}^r$ and s are learnable scalars.

Instead of training new models, Tang et al. [64] propose to utilize a mixture of experts [96] to combine pre-existing models in order to achieve the Pareto set. Given n models, $\theta_1, \dots, \theta_n$, each trained on different datasets, they are first integrated to a unified base model θ_0 . For some modules in the network, differences between the individual models and the base model (i.e., $\theta_i - \theta_0$'s) are maintained. These differences are treated as experts within the framework. Then, a mixture of experts is applied, where a gating network conditioned on user preferences determines the weighting of these experts. It enables the generation of diverse models by applying different weighted combinations of experts to align with specific user preferences.

5.2 Training Strategy

This section outlines the training approach for the parameters (denoted ϕ) of the network structures introduced in Section 5.1. Specifically, ϕ refers to the parameters of the Hypernetwork in Section 5.1.1, parameters of the preference-conditioned network in Section 5.1.2, or parameters of the

base models or low-rank models in Section 5.1.3. Current algorithms follow a similar approach: sample user preferences and optimize the structure parameters to generate networks that align with those preferences. The training objective can be written as:

$$\min_{\phi} \mathbb{E}_{\alpha \sim \Delta_{m-1}} \mathbb{E}_{(x, y) \sim \mathcal{D}} [\tilde{g}_{\alpha}(\ell(t(x; \theta(\alpha; \phi), y)))] , \quad (38)$$

where (x, y) 's are training data sampled from dataset \mathcal{D} , $\ell(\cdot, \cdot)$ is the multi-objective loss function and $\tilde{g}_{\alpha}(\cdot)$ is an MOO algorithm that produces a single solution given preference vector α . In general, most optimization algorithms discussed in Sections 2.2 and 4 can be adopted. Below, we summarize the algorithms adopted by the existing methods.

- **Scalarization:** As outlined in Section 2.2, scalarization combines multiple objectives into one scalar objective. Linear scalarization is common in most algorithms, such as PHN [52], COSMOS [57], PAMAL [60], and LORPMAN [61]. Alternatives like Tchebycheff and smooth Tchebycheff scalarization [18] can also be adopted.
- **Preference-Aware Weighting Methods:** As discussed in Section 4.1, these methods incorporate user preferences into optimization. PHN [52] employs the Exact Pareto Optimal (EPO) solver [37] to find Pareto-optimal solutions aligned with preferences. CPMTL [53] uses a constrained approach inspired by PMTL [36].
- **Hypervolume Maximization:** As discussed in Section 4.2, hypervolume maximization can optimize both diversity and convergence of a solution set. PHN-HVI [54] leverages hypervolume maximization to optimize the structural parameters ϕ . In each iteration, it samples a set of preference vectors and generates solutions based on these vectors. Subsequently, hypervolume maximization is applied to promote both the diversity and convergence of the solutions.

5.3 Discussions

Selecting the appropriate structural framework and optimization algorithms is important for effectively learning an infinite Pareto set. Hypernetwork-based approaches offer significant flexibility by generating a diverse set of models tailored to varying user preferences. However, their main drawback is size: the output dimension matches the target network's parameters, making hypernetworks significantly larger than base models. This limits their applicability for large-scale networks or resource-constrained scenarios.

In contrast, methods based on preference-conditioned networks are highly parameter-efficient. They introduce a minimal number of additional parameters relative to the base model, making them well-suited for large-scale applications where adding extra parameters is costly. However, their limited parameter space may reduce diversity, hindering their ability to approximate complex PS accurately.

Methods based on model combinations serve as a middle ground between hypernetwork and preference-conditioned network methods. By integrating multiple models, they offer a good approximation of the PS while maintaining scalability for large models. Furthermore, some methods allow for parameter adjustments through the selection of appropriate ranks in low-rank approximations.

TABLE 2: Convergence of existing stochastic gradient MOO algorithms. "LS" and "GS" denote the objectives are L -smooth and generalized L -smooth, respectively. "BG" and "BF" represent the bounded gradient and bounded function value assumptions, respectively. "Complexity" denotes the sample complexity achieving ϵ -accurate Pareto stationary point. "Bounded CA" denotes the bounded conflict-avoidant distance.

Method	Batch Size	Assumption	Complexity	Bounded CA
SMG [20]	$\mathcal{O}(\epsilon^{-2})$	LS, BG	$\mathcal{O}(\epsilon^{-4})$	✗
CR-MOGM [21]	$\mathcal{O}(1)$	LS, BF, BG	$\mathcal{O}(\epsilon^{-2})$	✗
MoCo [22]	$\mathcal{O}(1)$	LS, BF, BG	$\mathcal{O}(\epsilon^{-2})$	✗
PSMGD [23]	$\mathcal{O}(1)$	LS, BF, BG	$\mathcal{O}(\epsilon^{-2})$	✗
MoDo [24]	$\mathcal{O}(1)$	LS, BG	$\mathcal{O}(\epsilon^{-2})$	✓
SDMGrad [25]	$\mathcal{O}(1)$	LS, BG	$\mathcal{O}(\epsilon^{-2})$	✓
SGSMGrad [26]	$\mathcal{O}(1)$	GS	$\mathcal{O}(\epsilon^{-2})$	✓

Regarding training strategies, most algorithms use linear scalarization for its simplicity and strong performance. However, when aligning solutions with user preferences is important, preference-dependent weighting schemes in Section 4.1 are more suitable. Additionally, to achieve HV-optimal solutions, HV-based optimization criteria in Section 4.2 can also be employed, as they better capture the PF by focusing on the dominated objective space volume.

6 THEORIES

6.1 Convergence of Gradient-Balancing Methods in Section 3.2

This section reviews the convergence analysis for gradient-balancing methods in Section 3.2. This is first examined under the deterministic gradient setting (i.e., full-batch gradient). Subsequently, it is analyzed under the stochastic gradient setting. Note that in non-convex MOO, convergence refers to reaching Pareto stationary (Definition 5).

6.1.1 Deterministic Gradient

With the use of deterministic gradients, it has shown that under mild conditions, MGDA [6] can converge to a Pareto-stationary point at a convergence rate of $\mathcal{O}(K^{-1/2})$ [97], where K is the number of iterations. This rate is comparable to that of single-objective optimization [98]. The fundamental idea is to assess the reduction in each individual objective function. When the current solution is not Pareto-stationary, it can be shown that the common descent direction \mathbf{d} identified by MGDA ensures an improvement of at least $\mathcal{O}(\|\mathbf{d}\|^2)$ in each objective, which mirrors the situation in single-objective optimization [97]. Therefore, the method used in single-objective optimization can be applied to prove the convergence. Furthermore, other algorithms such as CAGrad [19], Nash-MTL [27], and PCGrad [33] also offer convergence analyses in similar approaches.

6.1.2 Stochastic Gradient

Liu and Vicente [20] are the first to analyze the convergence of gradient-based MOO algorithms with stochastic gradients. They propose a stochastic version of MGDA [6] that computes a common descent direction using stochastic gradients for all objectives and prove convergence to Pareto-optimal solutions under the assumption of convex objective

functions. However, due to the inherent bias of common descent direction \mathbf{d} introduced by stochastic gradient estimations, their analysis requires the use of an increasing batch size that grows linearly with the number of iterations to ensure convergence. This requirement can be impractical in real-world applications, as large batch sizes lead to increased computational costs and memory usage.

To overcome this limitation, Zhou et al. [21] propose Correlation-Reduced Stochastic Multi-Objective Gradient Manipulation (CR-MOGM). It addresses the bias in the common descent direction by introducing a smoothing technique on weight coefficient λ . In CR-MOGM, $\lambda^{(k)}$ at iteration k is updated using a moving average:

$$\lambda^{(k)} = (1 - \gamma)\hat{\lambda}^{(k)} + \gamma\lambda^{(k-1)}, \quad (39)$$

where $\gamma \in [0, 1]$ is a smoothing factor, $\hat{\lambda}^{(k)}$ is the weight vector obtained by the MOO solver (such as MGDA) at iteration k using the current stochastic gradients, and $\lambda^{(k-1)}$ is the smoothed weight from the previous iteration. Smoothing reduces the variance in the weight, leading to a more stable and reliable common descent direction. Xu et al. [23] further analyze the convergence by updating the objective weights every τ iterations instead of at each iteration, and achieve the same convergence rate $\mathcal{O}(\epsilon^{-2})$ as CR-MOGM. They also match the convergence rate in stochastic single-objective optimization [99].

Another approach to address gradient bias is MoCo [22], which introduces a tracking variable $\hat{\mathbf{g}}_i^{(k)}$ that approximates the true gradient:

$$\hat{\mathbf{g}}_i^{(k+1)} = \prod_{L_i} \left(\hat{\mathbf{g}}_i^{(k)} - \gamma \left(\hat{\mathbf{g}}_i^{(k)} - \mathbf{g}_i^{(k)} \right) \right), \quad (40)$$

where \prod_{L_i} is the projection to the set $\{\mathbf{g} \in \mathbb{R}^d \mid \|\mathbf{g}\| \leq L_i\}$, and L_i is the Lipschitz constant of $f_i(\theta)$. However, the analysis requires the number of iterations K to be sufficiently large (in the order of $\mathcal{O}(m^{10})$). This high dependency on m makes MoCo less practical for problems involving many objectives. Additionally, the convergence analysis of CR-MOGM and MoCo relies on the assumption that the objective functions have bounded values.

To address these limitations, Chen et al. [24] propose the Multi-objective gradient with double sampling algorithm (MoDo). MoDo mitigates bias in stochastic gradient-based MOO methods without assuming bounded function values. It introduces a double sampling technique to obtain unbiased estimates of the gradient products needed for updating the weight coefficients. Specifically, at each iteration, MoDo updates the weight vector $\lambda^{(k)}$ using gradients computed on two independent mini-batches:

$$\lambda^{(k+1)} = \prod_{\Delta_{m-1}} \left(\lambda^{(k)} - \eta \mathbf{G}^{(k)}(\mathbf{z}_1^{(k)})^\top \mathbf{G}^{(k)}(\mathbf{z}_2^{(k)}) \lambda^{(k)} \right), \quad (41)$$

where η is the step size, $\prod_{\Delta_{m-1}}$ is the projection onto the simplex Δ_{m-1} , and $\mathbf{G}^{(k)}(\mathbf{z}_1^{(k)})$, $\mathbf{G}^{(k)}(\mathbf{z}_2^{(k)})$ are stochastic gradients evaluated on two independent mini-batches $\mathbf{z}_1^{(k)}$ and $\mathbf{z}_2^{(k)}$. By reducing the bias in estimating the common descent direction, MoDo achieves convergence guarantees without the bounded function value assumption. Additionally, it guarantees a bounded conflict-avoidant (CA) dis-

tance, which is the distance between the estimated update direction and the CA direction defined in problem (12).

Similarly, Xiao et al. [25] propose the Stochastic Direction-oriented Multi-objective Gradient descent (SDM-Grad) algorithm, which introduces a new direction-oriented multi-objective formulation by regularizing the common descent direction within a neighborhood of a target direction (such as the average gradient of all objectives). In SDMGrad, the weight vector $\lambda^{(k)}$ is updated as:

$$\lambda^{(k+1)} = \prod_{\Delta_{m-1}} \left(\lambda^{(k)} - \eta \left[\mathbf{G}^{(k)}(\mathbf{z}_1^{(k)})^\top \left(\mathbf{G}^{(k)}(\mathbf{z}_2^{(k)}) \lambda^{(k)} + \gamma \mathbf{g}_0(\mathbf{z}_2^{(k)}) \right) \right] \right), \quad (42)$$

where η is the step size, γ is a regularization factor controlling the proximity to the target direction $\mathbf{g}_0(\mathbf{z}_2^{(k)})$. By incorporating this regularization, SDMGrad effectively balances optimization across objectives while guiding the overall descent direction. Zhang et al. [26] further consider the convergence under generalized L -smoothness [100] and without bounded gradient assumption. A summary of the convergence results of existing stochastic gradient MOO algorithms is provided in Table 2.

6.2 Generalization

The generalization aspect of multi-objective deep learning remains relatively underexplored compared to its convergence properties. Cortes et al. [101] analyze the generalization behavior of a specific scalarization approach that minimizes over convex combinations. Sukenik et al. [102] consider a broader class of scalarization methods. They show that the generalization bounds for individual objectives extend to MOO with scalarization. Both studies rely on the Rademacher complexity of the hypothesis class to establish algorithm-independent generalization bounds, which are unaffected by the training process.

Another line of research investigates Tchebycheff scalarization, which focuses on the sample complexity required to achieve a generalization error within ϵ of the optimal objective value. Formally, given a set of m distributions $\{\mathcal{D}_i\}_{i=1}^m$ and a hypothesis class \mathcal{H} , the goal is to find a (possibly randomized) hypothesis h such that

$$\max_{i \in [m]} \ell_{\mathcal{D}_i}(h) \leq \min_{h^* \in \mathcal{H}} \max_{i \in [m]} \ell_{\mathcal{D}_i}(h^*) + \epsilon, \quad (43)$$

where $\ell_{\mathcal{D}_i}(h)$ is the loss of hypothesis h on \mathcal{D}_i , h^* is the optimal hypothesis and ϵ is the error tolerance. It is first formulated by Awasthi et al. [103] as an open problem in 2023 and has since been addressed by several works [104], [105]. Haghtalab et al. are the first to show the sample complexity lower bound of $\tilde{\Omega}\left(\frac{v+m}{\epsilon^2}\right)$, where $v = \text{VCdim}(\mathcal{H})$ is the VC-dimension of the hypothesis class \mathcal{H} . By using a boosting framework, Peng [104] gives an algorithm that achieves a sample complexity upper bound of $\tilde{O}\left(\frac{v+m}{\epsilon^2} \cdot \left(\frac{m}{\epsilon}\right)^{o(1)}\right)$, which is nearly optimal. In a concurrent work, Zhang et al. [105] provide a variant of the hedge algorithm under an Empirical Risk Minimization (ERM) oracle access that achieves the optimal sample complexity bound of $\tilde{O}\left(\frac{v+m}{\epsilon^2}\right)$.

In the online setting, Liu et al. [106] provide an adaptive online mirror descent algorithm that achieves $\mathcal{O}\left(\frac{mv}{\sqrt{K}}\right)$

regret, where K is the number of iterations. Using a plain online-to-batch conversion scheme, this algorithm leads to an $\mathcal{O}\left(\frac{m^2 v^2}{\epsilon^2}\right)$ sample complexity, which still lags behind the optimal offline sample complexity of $\tilde{\mathcal{O}}\left(\frac{m+v}{\epsilon^2}\right)$ [105]. It is interesting to see whether it is possible to use an online learner with proper online-to-batch conversion schemes that is able to match the optimal offline sample complexity.

MoDo [24] introduces a different perspective by leveraging algorithm stability to derive algorithm-dependent generalization error bounds of gradient balancing algorithms.

7 APPLICATIONS

7.1 Reinforcement Learning

Reinforcement Learning (RL) [107] involves training agents to make sequential decisions by maximizing cumulative rewards. Multi-Objective Reinforcement Learning (MORL) [108] extends single-objective RL by utilizing a vector-valued reward function $r(s, a) : \mathcal{S} \times \mathcal{A} \mapsto \mathbb{R}^m$. MORL aims to learn a policy network $\pi_\theta(s)$ with the following training objective:

$$\min_{\theta} \mathbf{f}(\theta) := \mathbb{E}_{a \sim \pi_\theta(s)} \sum_{t=1}^{\infty} \gamma^t r(s_t, a_t), \quad (44)$$

where t is the time step and γ^t is the discount factor.

Radius Algorithm (RA) [109] employs linear scalarization with fixed preference vectors to transform a MORL problem into a single-objective RL problem. However, a uniform distribution of preferences does not always lead to a uniform distribution of solutions. To address this, various methods focus on improving the configuration of preference vectors. For instance, Optimal Linear Support (OLS) [110], [111] adds new preference vectors dynamically during each iteration. Prediction-guided MORL (PGMORL) [112] employs a hyperbolic model to map preference vectors to objective values, periodically updating preference vectors to optimize both the hypervolume and a diversity indicator.

Although Lu et al. [5] demonstrated that linear scalarization can recover the entire PS when the policy space includes all stochastic policies, this assumption may be too strong in practice, necessitating approaches beyond naive linear scalarization. CAPQL [113] introduces a scalarization method that combines linear scalarization with an entropy term. PPA [114] incorporates a term to align objective values more closely with preference vectors. Several studies [115]–[120] have explored other scalarization functions, such as the Tchebycheff function, to identify Pareto-optimal policies. Beyond scalarization, gradient balancing methods (discussed in Section 3.2) also demonstrate promising performance in MORL.

Another research direction focuses on learning the entire Pareto set [121]–[126]. In these approaches, the policy network $\pi_\theta(s, \alpha)$ is conditioned on both the state s and preference vector α . Most of these methods employ training strategies similar to those described in Section 5.2, but with an RL-specific training objective.

7.2 Bayesian Optimization

Bayesian Optimization (BO) [127] is a framework for optimizing expensive-to-evaluate black-box functions by using

a probabilistic surrogate model. When extended to handle multiple black-box objectives simultaneously, this approach is known as Multi-Objective Bayesian Optimization (MOBO) [128]. In MOBO, acquisition functions are designed to manage the balance between exploration and exploitation across *multiple* objectives. Based on this, MOBO methods can be classified into three main categories:

- 1) **Scalarization-based Methods.** These methods convert MOO problems into single-objective ones using scalarization functions discussed in Section 2.2 [128], [129]. Zhang and Golovin [130] propose using the hypervolume indicator for scalarization. Instead of scalarizing first and then applying single-objective acquisition functions, methods like SMS-EGO [131], PAL [132], [133], and MOBO-RS [134] extend single-objective acquisitions to multi-objective optimization.
- 2) **Hypervolume Improvement-Based Methods.** These methods extend Expected Improvement (EI) [135] to Expected Hypervolume Improvement (EHVI) [136], which selects candidate points to enhance the current solution set’s hypervolume. Many algorithms are proposed to improve the efficiency and allow parallel candidate generation [137]–[144].
- 3) **Information Theoretic-Based Methods.** These methods aim to maximize information gain about the PF by selecting candidate points. PESMO [145] reduces uncertainty in the posterior over the Pareto optimal input set. Some extensions [146]–[149] refine this by considering output space. USEMO [150] offers an alternative uncertainty measure based on hyper-rectangle volumes.

The solutions obtained by the aforementioned methods provide discrete approximations of the Pareto set. Lin et al. [151] propose learning a continuous approximation of the Pareto set in MOBO using a hypernetwork (introduced in Section 5.1.1). Subsequent improvements have been proposed to leverage diffusion models [152] and Stein variational gradient descent [153] for efficient solution generation, as well as incorporating data augmentation for Pareto set model building [154].

7.3 Computer Vision

The most representative application of MOO in computer vision is multi-task dense prediction [4], which aims to train a model for simultaneously dealing with multiple dense prediction tasks (such as semantic segmentation, monocular depth estimation, and surface normal estimation) and has been successfully applied in autonomous driving [155], [156]. Since the encoder in computer vision usually contains large number of parameters, sharing the encoder across different tasks can significantly reduce the computational cost but may cause conflicts among tasks, leading to a performance drop in some of the tasks. Hence, many methods are proposed to address the issue from the perspective of MOO, which use scalarization to balance multiple losses [157]–[161]. A comprehensive survey on multi-task dense prediction is in [4].

Besides the dense prediction task, MOO is also useful in other computer vision tasks such as point cloud [162]–[164], medical image denoising [165], and pose estimation [166].

7.4 Neural Architecture Search

Neural Architecture Search (NAS), which aims to design the architecture of neural networks automatically, has gained significant interest recently [167]. Due to the complex application scenarios in the real world, recent works consider multiple objectives beyond just accuracy. For example, to search an efficient architecture for deployment on platforms with limited resources, many studies incorporate resource-constraint objectives such as the parameter size, FLOPs, and latency. These works are mainly based on gradient-based NAS methods (like DARTS [168]) and formulate it as a multi-objective optimization problem. Among them, [8], [169]–[172] employ scalarization to identify a single solution, where the task and efficiency objectives are combined with fixed weights. However, altering the weights of the objectives needs a complete rerun of the search, which is computationally intensive. Therefore, Sukthanker et al. [173] propose to learn a mapping from a preference vector to an architecture using a hypernetwork, enabling to provide the entire PS without the need for a new search.

7.5 Recommendation System

Beyond just focusing on accuracy, recommendation systems often incorporate additional quality metrics such as novelty, diversity, serendipity, popularity, and others [174]. These factors naturally frame the problem as a multi-objective optimization optimization. Traditionally, many methods have employed scalarization techniques to assign weights to the different objectives [175]–[177]. In recent developments, gradient-balancing approaches are applied to address multi-objective optimization within recommendation systems to learn a single recommendation model [178]–[181]. Additionally, some research efforts aim to identify finite Pareto sets [182] and infinite Pareto sets [183], [184], enabling the provision of personalized recommender models that cater to varying user preferences.

7.6 Large Language Models (LLMs)

Recently, there has been a growing trend of incorporating multi-objective optimization into the training of large language models (LLMs), including multi-task fine-tuning and multi-objective alignment.

Due to the powerful transferability of LLMs, users can fine-tune LLMs to specific downstream tasks or scenarios. This approach separates fine-tuning on each task, causing extensive costs in training and difficulties in deployment. MFTCoder [185] proposes a multi-task fine-tuning framework that enhances the coding capabilities of LLMs by addressing data imbalance, varying difficulty levels, and inconsistent convergence speeds across tasks. CoBa [186] studies multi-task fine-tuning for LLMs and balances task convergence with minimal computational overhead.

Aligning with multi-dimensional human preferences (such as helpfulness, harmfulness, humor, and conciseness) is essential for customizing responses to users’ needs, as users typically have diverse preferences for different aspects. MORLHF [187] and MODPO [188] train an LLM for every preference configuration by linearly combining multiple (implicit) reward models. To avoid retraining, some

TABLE 3: Summary of benchmark datasets in multi-objective deep learning.

Dataset	Description	#Objectives	#Samples
NYUv2 [219]	indoor scene understanding	3	1, 449
Taskonomy [220]	indoor scene understanding	26	≈ 4M
Cityscapes [221]	urban scene understanding	2	3, 475
QM9 [222]	molecular property prediction	11	130K
Office-31 [223]	image classification	3	4, 110
Office-Home [224]	image classification	4	15, 500
CelebA [225]	image classification	40	≈ 202K
CIFAR-100 [226]	image classification	20	60K
MT10/MT50 [227]	reinforcement learning	10/50	-
XTREME [228]	multilingual learning	9	≈ 597K
PKU-SafeRLHF [229]	two-dimensional preference data	2	≈ 82K
UltraFeedBack [230]	multi-dimensional preference data	4	≈ 64K
HelpSteer2 [231]	multi-attributes preference data	5	≈ 21K

methods train multiple LLMs separately for each preference dimension and merge their parameters [189], [190] or output logits [191] to deal with different preference requirements. However, these methods need to train and store multiple LLMs, leading to huge computational and storage costs. To improve efficiency, several preference-aware methods are proposed to fine-tune a single LLM for varying preferences by incorporating the relevant coefficients into the input prompts [192]–[194] or model parameters [63].

7.7 Miscellaneous

In addition to the applications mentioned above, multi-objective optimization has been applied to a variety of other deep learning scenarios, including meta-learning [195], [196], federated learning [197]–[199], long-tailed learning [200]–[202], continual learning [203], diffusion models [204]–[207], neural combinatorial optimization [122], [208]–[211], GFlowNets [212], [213], and physics informed neural networks (PINNs) [214], [215]. These applications highlight the versatility of multi-objective optimization in addressing diverse challenges within deep learning.

8 RESOURCES

In this section, we introduce some benchmark datasets and open-source libraries for gradient-based MOO in deep learning. Benchmark datasets are summarized in Table 3, with details in Appendix C.

Two popular libraries, LibMTL¹ [216] and LibMOON² [217], provide unified environments for implementing and fairly evaluating MOO methods. Both are built on PyTorch [218] and feature modular designs, enabling flexible development of new methods or application of existing ones to new scenarios. LibMTL [216] mainly focuses on finding a single Pareto-optimal solution and supports 24 methods introduced in Section 3 and 6 benchmark datasets. LibMOON [217] mainly focuses on exploring the whole Pareto set. It includes over 20 methods for obtaining a finite set of solutions (introduced in Section 4) or infinite set of solutions (introduced in Section 5).

9 CHALLENGES AND FUTURE DIRECTIONS

Despite significant progress in applying MOO in deep learning, both in learning a single model and in learning a Pareto set of models, several challenges remain.

1. <https://github.com/median-research-group/LibMTL>
2. <https://github.com/xzhang2523/libmoon>

Theoretical Understanding. While practical methods for MOO in deep learning have seen significant progress, their theoretical foundations remain relatively underexplored.

Most existing research focuses on analyzing the convergence of MOO algorithms to stationary points, while generalization error, which is critical for evaluating performance on unseen data, has received less attention. For instance, Chen et al. [24], as discussed in Section 6.2, provide the algorithm-dependent generalization analysis. Extending this to a broader range of algorithms could offer deeper insights into how different techniques affect generalization.

For Pareto set learning algorithms, there is limited theoretical understanding of how effectively existing algorithms can approximate Pareto sets. Zhang et al. [232] established a generalization bound for HV-based Pareto set learning. However, the effect of various network architectures (Section 5.1) on approximating Pareto sets remain unclear. Additionally, it is uncertain how effective current training strategies (Section 5.2) are in approximating the Pareto set.

Reducing Gradient Balancing Costs. While gradient balancing methods in Section 3.2 often show strong performance in various applications, they come with significant computational overhead. Despite the introduction of some practical speedup strategies (discussed in Section 3.2.3), existing approaches remain insufficiently efficient. A deeper understanding of the optimization differences between gradient balancing, linear scalarization, and loss balancing is crucial. This insight could facilitate the integration of gradient balancing with linear scalarization and loss balancing, reducing computational overhead significantly and enabling its application in large-scale training scenarios.

Dealing with Large Number of Objectives. Some real-world problems involve handling a large number of objectives, which poses significant challenges for current Pareto set learning algorithms in Section 5. As the number of objectives grows, the preference vector space expands exponentially, making it challenging for existing random sampling-based techniques to effectively learn the mapping between preference vectors and solutions. Developing efficient sampling strategies for high-dimensional preference spaces remains a important research problem. Additionally, exploring methods to reduce or merge objectives based on their properties can be a promising approach to minimize the total number of objectives.

Distributed Training. Current MOO algorithms in deep learning are limited to single GPUs or machines, but scaling them to multi-GPU and distributed environments is increasingly important as models and datasets grow. This scaling introduces unique challenges compared to single-objective optimization. Gradient-balancing algorithms require efficient gradient distribution and communication across GPUs. Learning a set of Pareto-optimal solutions involves synchronizing multiple models across nodes with minimal overhead. Additionally, when data for different objectives is distributed across devices and cannot be shared (e.g., due to privacy constraints), collaborative computation of solutions or Pareto sets without direct data sharing becomes an important challenge.

Advancements in Large Language Models (LLMs). As

discussed in Section 7.6, current research in MOO for LLMs largely focuses on the RLHF stage. Expanding MOO techniques to other stages in the LLM lifecycle, such as pre-training and inference, is a valuable direction for future research. Addressing these challenges can lead to models that are better aligned with user needs across their entire development processes. Additionally, user preferences are currently modeled as a preference vector. However, this representation may oversimplify more complex user preferences on LLMs. Exploring advanced methods to capture and represent these intricate preferences can enhance the effectiveness and personalization of LLMs.

Application in More Deep Learning Scenarios. While MOO has already been utilized in various deep learning scenarios, as highlighted in Section 7, there remain numerous unexplored areas within this field. Multi-objective characteristics are inherently present in most deep learning problems, as models are typically developed or evaluated based on multiple criteria. Consequently, trade-offs often arise naturally. Leveraging MOO methods to effectively address these trade-offs presents an opportunity for further exploration.

10 CONCLUSION

In this paper, we provide the first comprehensive review of gradient-based MOO in deep learning, covering algorithms, theoretical foundations, applications, benchmark datasets, and software. By unifying diverse approaches and systematically identifying key challenges, this paper serves as a foundational resource to drive future advancements in this important and evolving field.

REFERENCES

- [1] K. Miettinen, *Nonlinear multiobjective optimization*. Springer Science & Business Media, 1999, vol. 12.
- [2] R. T. Marler and J. S. Arora, "Survey of multi-objective optimization methods for engineering," *Structural and Multidisciplinary Optimization*, vol. 26, pp. 369–395, 2004.
- [3] Y. Zhang and Q. Yang, "A survey on multi-task learning," *IEEE Transactions on Knowledge and Data Engineering*, vol. 34, no. 12, pp. 5586–5609, 2021.
- [4] S. Vandenhende, S. Georgoulis, W. Van Gansbeke, M. Proesmans, D. Dai, and L. Van Gool, "Multi-task learning for dense prediction tasks: A survey," *IEEE Transactions on Pattern Analysis and Machine Intelligence*, vol. 44, no. 7, pp. 3614–3633, 2021.
- [5] H. Lu, D. Herman, and Y. Yu, "Multi-objective reinforcement learning: Convexity, stationarity and Pareto optimality," in *ICLR*, 2023.
- [6] O. Sener and V. Koltun, "Multi-task learning as multi-objective optimization," in *NeurIPS*, 2018.
- [7] Y. Wang, W. Zhong, L. Li, F. Mi, X. Zeng, W. Huang, L. Shang, X. Jiang, and Q. Liu, "Aligning large language models with human: A survey," *arXiv preprint arXiv:2307.12966*, 2023.
- [8] B. Wu, X. Dai, P. Zhang, Y. Wang, F. Sun, Y. Wu, Y. Tian, P. Vajda, Y. Jia, and K. Keutzer, "FBNet: Hardware-aware efficient convnet design via differentiable neural architecture search," in *CVPR*, 2019.
- [9] S. Liu, E. Johns, and A. J. Davison, "End-to-end multi-task learning with attention," in *CVPR*, 2019.
- [10] A. Kendall, Y. Gal, and R. Cipolla, "Multi-task learning using uncertainty to weigh losses for scene geometry and semantics," in *CVPR*, 2018.
- [11] L. Liu, Y. Li, Z. Kuang, J.-H. Xue, Y. Chen, W. Yang, Q. Liao, and W. Zhang, "Towards impartial multi-task learning," in *ICLR*, 2021.

- [12] B. Lin, W. Jiang, F. Ye, Y. Zhang, P. Chen, Y.-C. Chen, S. Liu, and J. T. Kwok, "Dual-balancing for multi-task learning," *arXiv preprint arXiv:2308.12029*, 2023.
- [13] F. Ye, B. Lin, Z. Yue, P. Guo, Q. Xiao, and Y. Zhang, "Multi-objective meta learning," in *NeurIPS*, 2021.
- [14] F. Ye, B. Lin, Z. Yue, Y. Zhang, and I. Tsang, "Multi-objective meta-learning," *Artificial Intelligence*, vol. 335, p. 104184, 2024.
- [15] S. Liu, S. James, A. Davison, and E. Johns, "Auto-Lambda: Disentangling dynamic task relationships," *Transactions on Machine Learning Research*, 2022.
- [16] F. Ye, B. Lin, X. Cao, Y. Zhang, and I. Tsang, "A first-order multi-gradient algorithm for multi-objective bi-level optimization," in *ECAL*, 2024.
- [17] B. Lin, F. Ye, Y. Zhang, and I. Tsang, "Reasonable effectiveness of random weighting: A litmus test for multi-task learning," *Transactions on Machine Learning Research*, 2022.
- [18] X. Lin, X. Zhang, Z. Yang, F. Liu, Z. Wang, and Q. Zhang, "Smooth tchebycheff scalarization for multi-objective optimization," in *ICML*, 2024.
- [19] B. Liu, X. Liu, X. Jin, P. Stone, and Q. Liu, "Conflict-averse gradient descent for multi-task learning," in *NeurIPS*, 2021.
- [20] S. Liu and L. N. Vicente, "The stochastic multi-gradient algorithm for multi-objective optimization and its application to supervised machine learning," *Annals of Operations Research*, pp. 1–30, 2021.
- [21] S. Zhou, W. Zhang, J. Jiang, W. Zhong, J. Gu, and W. Zhu, "On the convergence of stochastic multi-objective gradient manipulation and beyond," in *NeurIPS*, 2022.
- [22] H. Fernando, H. Shen, M. Liu, S. Chaudhury, K. Murugesan, and T. Chen, "Mitigating gradient bias in multi-objective learning: A provably convergent approach," in *ICLR*, 2023.
- [23] M. Xu, P. Ju, J. Liu, and H. Yang, "PSMGD: Periodic stochastic multi-gradient descent for fast multi-objective optimization," in *AAAI*, 2025.
- [24] L. Chen, H. Fernando, Y. Ying, and T. Chen, "Three-way trade-off in multi-objective learning: Optimization, generalization and conflict-avoidance," in *NeurIPS*, 2023.
- [25] P. Xiao, H. Ban, and K. Ji, "Direction-oriented multi-objective learning: Simple and provable stochastic algorithms," in *NeurIPS*, 2023.
- [26] Q. Zhang, P. Xiao, K. Ji, and S. Zou, "MGDA converges under generalized smoothness, provably," in *ICLR*, 2025.
- [27] A. Navon, A. Shamsian, I. Achituve, H. Maron, K. Kawaguchi, G. Chechik, and E. Fetaya, "Multi-task learning as a bargaining game," in *ICML*, 2022.
- [28] H. Ban and K. Ji, "Fair resource allocation in multi-task learning," in *ICML*, 2024.
- [29] P. Quinton and V. Rey, "Jacobian descent for multi-objective optimization," *arXiv preprint arXiv:2406.16232*, 2024.
- [30] D. Senushkin, N. Patakin, A. Kuznetsov, and A. Konushin, "Independent component alignment for multi-task learning," in *CVPR*, 2023.
- [31] Z. Chen, V. Badrinarayanan, C.-Y. Lee, and A. Rabinovich, "Grad-Norm: Gradient normalization for adaptive loss balancing in deep multitask networks," in *ICML*, 2018.
- [32] B. Liu, Y. Feng, P. Stone, and Q. Liu, "FAMO: Fast adaptive multitask optimization," in *NeurIPS*, 2023.
- [33] T. Yu, S. Kumar, A. Gupta, S. Levine, K. Hausman, and C. Finn, "Gradient surgery for multi-task learning," in *NeurIPS*, 2020.
- [34] Z. Wang, Y. Tsvetkov, O. Firat, and Y. Cao, "Gradient vaccine: Investigating and improving multi-task optimization in massively multilingual models," in *ICLR*, 2021.
- [35] Z. Chen, J. Ngiam, Y. Huang, T. Luong, H. Kretschmar, Y. Chai, and D. Anguelov, "Just pick a sign: Optimizing deep multitask models with gradient sign dropout," in *NeurIPS*, 2020.
- [36] X. Lin, H.-L. Zhen, Z. Li, Q.-F. Zhang, and S. Kwong, "Pareto multi-task learning," in *NeurIPS*, 2019.
- [37] D. Mahapatra and V. Rajan, "Multi-task learning with user preferences: Gradient descent with controlled ascent in Pareto optimization," in *ICML*, 2020.
- [38] —, "Exact Pareto optimal search for multi-task learning and multi-criteria decision-making," *arXiv preprint arXiv:2108.00597*, 2021.
- [39] M. Momma, C. Dong, and J. Liu, "A multi-objective/multi-task learning framework induced by Pareto stationarity," in *ICML*, 2022.
- [40] X. Zhang, X. Lin, and Q. Zhang, "PMGDA: A preference-based multiple gradient descent algorithm," *IEEE Transactions on Emerging Topics in Computational Intelligence*, 2024.
- [41] L. Chen, A. Saif, Y. Shen, and T. Chen, "FERERO: A flexible framework for preference-guided multi-objective learning," in *NeurIPS*, 2024.
- [42] W. Chen and J. Kwok, "Multi-objective deep learning with adaptive reference vectors," in *NeurIPS*, 2022.
- [43] X. Zhang, G. Li, X. Lin, Y. Zhang, Y. Chen, and Q. Zhang, "Gliding over the Pareto front with uniform designs," in *NeurIPS*, 2024.
- [44] T. M. Deist, M. Grewal, F. J. Dankers, T. Alderliesten, and P. A. Bosman, "Multi-objective learning to predict Pareto fronts using hypervolume maximization," *arXiv preprint arXiv:2102.04523*, 2021.
- [45] T. M. Deist, S. C. Maree, T. Alderliesten, and P. A. Bosman, "Multi-objective optimization by uncrowded hypervolume gradient ascent," in *PPSN*, 2020.
- [46] M. Emmerich, A. Deutz, and N. Beume, "Gradient-based/evolutionary relay hybrid for computing Pareto front approximations maximizing the s-metric," in *Hybrid Metaheuristics: 4th International Workshop*, 2007.
- [47] H. Wang, A. Deutz, T. Bäck, and M. Emmerich, "Hypervolume indicator gradient ascent multi-objective optimization," in *EMO*, 2017.
- [48] X. Liu, X. Tong, and Q. Liu, "Profiling Pareto front with multi-objective stein variational gradient descent," in *NeurIPS*, 2021.
- [49] X. Lin, Y. Liu, X. Zhang, F. Liu, Z. Wang, and Q. Zhang, "Few for many: Tchebycheff set scalarization for many-objective optimization," in *ICLR*, 2025.
- [50] L. Ding, Z. Chen, X. Wang, and W. Yin, "Efficient algorithms for sum-of-minimum optimization," in *ICML*, 2024.
- [51] Z. Li, T. Li, V. Smith, J. Bilmes, and T. Zhou, "Many-objective multi-solution transport," in *ICLR*, 2025.
- [52] A. Navon, A. Shamsian, E. Fetaya, and G. Chechik, "Learning the Pareto front with hypernetworks," in *ICLR*, 2021.
- [53] X. Lin, Z. Yang, Q. Zhang, and S. Kwong, "Controllable Pareto multi-task learning," *arXiv preprint arXiv:2010.06313*, 2020.
- [54] L. P. Hoang, D. D. Le, T. A. Tuan, and T. N. Thang, "Improving Pareto front learning via multi-sample hypernetworks," in *AAAI*, 2023.
- [55] S. Gupta, G. Singh, R. Bollapragada, and M. Lease, "Learning a neural Pareto manifold extractor with constraints," in *UAI*, 2022.
- [56] T. A. Tuan, N. V. Dung, and T. N. Thang, "A hyper-transformer model for controllable Pareto front learning with split feasibility constraints," *arXiv preprint arXiv:2402.05955*, 2024.
- [57] M. Ruchte and J. Grabocka, "Scalable Pareto front approximation for deep multi-objective learning," in *ICDM*, 2021.
- [58] A. Dosovitskiy and J. Djonlaga, "You only train once: Loss-conditional training of deep networks," in *ICLR*, 2020.
- [59] D. S. Raychaudhuri, Y. Suh, S. Schuler, X. Yu, M. Faraki, A. K. Roy-Chowdhury, and M. Chandraker, "Controllable dynamic multi-task architectures," in *CVPR*, 2022.
- [60] N. Dimitriadis, P. Frossard, and F. Fleuret, "Pareto manifold learning: Tackling multiple tasks via ensembles of single-task models," in *ICML*, 2023.
- [61] W. Chen and J. Kwok, "Efficient Pareto manifold learning with low-rank structure," in *ICML*, 2024.
- [62] —, "You only merge once: Learning the Pareto set of preference-aware model merging," *arXiv preprint arXiv:2408.12105*, 2024.
- [63] Y. Zhong, C. Ma, X. Zhang, Z. Yang, Q. Zhang, S. Qi, and Y. Yang, "Panacea: Pareto alignment via preference adaptation for LLMs," in *NeurIPS*, 2024.
- [64] A. Tang, L. Shen, Y. Luo, S. Liu, H. Hu, and B. Du, "Towards efficient Pareto set approximation via mixture of experts based model fusion," *arXiv preprint arXiv:2406.09770*, 2024.
- [65] N. Dimitriadis, P. Frossard, and F. Fleuret, "Pareto low-rank adapters: Efficient multi-task learning with preferences," in *ICLR*, 2025.
- [66] M. Crawshaw, "Multi-task learning with deep neural networks: A survey," *arXiv preprint arXiv:2009.09796*, 2020.
- [67] J. Yu, Y. Dai, X. Liu, J. Huang, Y. Shen, K. Zhang, R. Zhou, E. Adhikarla, W. Ye, Y. Liu *et al.*, "Unleashing the power of multi-task learning: A comprehensive survey spanning traditional, deep, and pretrained foundation model eras," *arXiv preprint arXiv:2404.18961*, 2024.

- [68] G. Eichfelder, "Twenty years of continuous multiobjective optimization in the twenty-first century," *EURO Journal on Computational Optimization*, vol. 9, p. 100014, 2021.
- [69] T. Wei, S. Wang, J. Zhong, D. Liu, and J. Zhang, "A review on evolutionary multitask optimization: Trends and challenges," *IEEE Transactions on Evolutionary Computation*, vol. 26, no. 5, pp. 941–960, 2021.
- [70] S. Peitz and S. S. Hotegni, "Multi-objective deep learning: Taxonomy and survey of the state of the art," *arXiv preprint arXiv:2412.01566*, 2024.
- [71] M. Zhang, R. Yin, Z. Yang, Y. Wang, and K. Li, "Advances and challenges of multi-task learning method in recommender system: a survey," *arXiv preprint arXiv:2305.13843*, 2023.
- [72] S. Chen, Y. Zhang, and Q. Yang, "Multi-task learning in natural language processing: An overview," *ACM Computing Surveys*, vol. 56, no. 12, pp. 1–32, 2024.
- [73] J.-A. Désidéri, "Multiple-gradient descent algorithm (MGDA) for multiobjective optimization," *Comptes Rendus Mathématique*, vol. 350, no. 5–6, pp. 313–318, 2012.
- [74] E. Zitzler and L. Thiele, "Multiobjective optimization using evolutionary algorithms—a comparative case study," in *PPSN*, 1998.
- [75] V. J. Bowman Jr, "On the relationship of the tchebycheff norm and the efficient frontier of multiple-criteria objectives," in *Multiple Criteria Decision Making: Proceedings of a Conference Jouy-en-Josas*, 1976.
- [76] R. E. Steuer and E.-U. Choo, "An interactive weighted tchebycheff procedure for multiple objective programming," *Mathematical Programming*, vol. 26, pp. 326–344, 1983.
- [77] E. U. Choo and D. R. Atkins, "Proper efficiency in nonconvex multicriteria programming," *Mathematics of Operations Research*, vol. 8, no. 3, pp. 467–470, 1983.
- [78] S. Rudner, "An overview of multi-task learning in deep neural networks," *arXiv preprint arXiv:1706.05098*, 2017.
- [79] T. Standley, A. Zamir, D. Chen, L. Guibas, J. Malik, and S. Savarese, "Which tasks should be learned together in multi-task learning?" in *ICML*, 2020.
- [80] R. Liu, X. Liu, X. Yuan, S. Zeng, and J. Zhang, "A value-function-based interior-point method for non-convex bi-level optimization," in *ICML*, 2021.
- [81] M. Jaggi, "Revisiting frank-wolfe: Projection-free sparse convex optimization," in *ICML*, 2013.
- [82] J. Nash, "Two-person cooperative games," *Econometrica: Journal of the Econometric Society*, pp. 128–140, 1953.
- [83] W. Thomson, "Cooperative models of bargaining," *Handbook of Game Theory with Economic Applications*, vol. 2, pp. 1237–1284, 1994.
- [84] R. Cheng, Y. Jin, M. Olhofer *et al.*, "Test problems for large-scale multiobjective and many-objective optimization," *IEEE Transactions on Cybernetics*, vol. 47, no. 12, pp. 4108–4121, 2016.
- [85] Q. Zhang and H. Li, "MOEA/D: A multiobjective evolutionary algorithm based on decomposition," *IEEE Transactions on Evolutionary Computation*, vol. 11, no. 6, pp. 712–731, 2007.
- [86] K. Shang, H. Ishibuchi, L. He, and L. M. Pang, "A survey on the hypervolume indicator in evolutionary multiobjective optimization," *IEEE Transactions on Evolutionary Computation*, vol. 25, no. 1, pp. 1–20, 2020.
- [87] N. Beume, C. M. Fonseca, M. Lopez-Ibanez, L. Paquete, and J. Vahrenhold, "On the complexity of computing the hypervolume indicator," *IEEE Transactions on Evolutionary Computation*, vol. 13, no. 5, pp. 1075–1082, 2009.
- [88] A. P. Guerreiro, C. M. Fonseca, M. T. Emmerich *et al.*, "A fast dimension-sweep algorithm for the hypervolume indicator in four dimensions." in *CCCG*, 2012.
- [89] V. A. Sosa Hernández, O. Schütze, H. Wang, A. Deutz, and M. Emmerich, "The set-based hypervolume newton method for bi-objective optimization," *IEEE Transactions on Cybernetics*, vol. 50, no. 5, pp. 2186–2196, 2020.
- [90] Q. Liu and D. Wang, "Stein variational gradient descent: A general purpose bayesian inference algorithm," in *NeurIPS*, 2016.
- [91] Y. Liu, C. Lu, X. Lin, and Q. Zhang, "Many-objective cover problem: Discovering few solutions to cover many objectives," in *PPSN*, 2024.
- [92] P. Ma, T. Du, and W. Matusik, "Efficient continuous Pareto exploration in multi-task learning," in *ICML*, 2020.
- [93] D. Ha, A. Dai, and Q. V. Le, "Hypernetworks," *arXiv preprint arXiv:1609.09106*, 2016.
- [94] E. Perez, F. Strub, H. De Vries, V. Dumoulin, and A. Courville, "FiLM: Visual reasoning with a general conditioning layer," in *AAAI*, 2018.
- [95] T. G. Kolda and B. W. Bader, "Tensor decompositions and applications," *SIAM review*, vol. 51, no. 3, pp. 455–500, 2009.
- [96] W. Cai, J. Jiang, F. Wang, J. Tang, S. Kim, and J. Huang, "A survey on mixture of experts," *arXiv preprint arXiv:2407.06204*, 2024.
- [97] J. Fliege, A. I. F. Vaz, and L. N. Vicente, "Complexity of gradient descent for multiobjective optimization," *Optimization Methods and Software*, vol. 34, no. 5, pp. 949–959, 2019.
- [98] Y. Nesterov, *Introductory lectures on convex optimization: A basic course*. Springer Science & Business Media, 2013, vol. 87.
- [99] S. Ghadimi and G. Lan, "Stochastic first-and zeroth-order methods for nonconvex stochastic programming," *SIAM Journal on Optimization*, vol. 23, no. 4, pp. 2341–2368, 2013.
- [100] H. Li, J. Qian, Y. Tian, A. Rakhlin, and A. Jadbabaie, "Convex and non-convex optimization under generalized smoothness," in *NeurIPS*, 2023.
- [101] C. Cortes, M. Mohri, J. Gonzalvo, and D. Storcheus, "Agnostic learning with multiple objectives," in *NeurIPS*, 2020.
- [102] P. Sükönik and C. Lampert, "Generalization in multi-objective machine learning," *Neural Computing and Applications*, pp. 1–15, 2024.
- [103] P. Awasthi, N. Haghtalab, and E. Zhao, "Open problem: The sample complexity of multi-distribution learning for vc classes," in *COLT*, 2023.
- [104] B. Peng, "The sample complexity of multi-distribution learning," in *COLT*, 2024.
- [105] Z. Zhang, W. Zhan, Y. Chen, S. S. Du, and J. D. Lee, "Optimal multi-distribution learning," in *COLT*, 2024.
- [106] M. Liu, X. Zhang, C. Xie, K. Donahue, and H. Zhao, "Online mirror descent for tchebycheff scalarization in multi-objective optimization," *arXiv preprint arXiv:2410.21764*, 2024.
- [107] X. Wang, S. Wang, X. Liang, D. Zhao, J. Huang, X. Xu, B. Dai, and Q. Miao, "Deep reinforcement learning: A survey," *IEEE Transactions on Neural Networks and Learning Systems*, vol. 35, no. 4, pp. 5064–5078, 2024.
- [108] F. Felten, E.-G. Talbi, and G. Danoy, "Multi-objective reinforcement learning based on decomposition: A taxonomy and framework," *Journal of Artificial Intelligence Research*, vol. 79, pp. 679–723, 2024.
- [109] S. Parisi, M. Pirotta, N. Smacchia, L. Bascetta, and M. Restelli, "Policy gradient approaches for multi-objective sequential decision making," in *IJCNN*, 2014.
- [110] D. M. Roijers, "Multi-objective decision-theoretic planning," *AI Matters*, vol. 2, no. 4, pp. 11–12, 2016.
- [111] D. M. Roijers, S. Whiteson, and F. A. Oliehoek, "Linear support for multi-objective coordination graphs," in *AAMAS*, 2014.
- [112] J. Xu, Y. Tian, P. Ma, D. Rus, S. Sueda, and W. Matusik, "Prediction-guided multi-objective reinforcement learning for continuous robot control," in *ICML*, 2020.
- [113] Y. Hu, R. Xian, Q. Wu, Q. Fan, L. Yin, and H. Zhao, "Revisiting scalarization in multi-task learning: A theoretical perspective," in *NeurIPS*, 2023.
- [114] P. Kyriakis and J. Deshmukh, "Pareto policy adaptation," in *ICLR*, 2022.
- [115] N. Peng and B. Fain, "Nonlinear multi-objective reinforcement learning with provable guarantees," *arXiv preprint arXiv:2311.02544*, 2023.
- [116] K. Van Moffaert, M. M. Drugan, and A. Nowé, "Scalarized multi-objective reinforcement learning: Novel design techniques," in *ADPRL*, 2013.
- [117] Q. Bai, M. Agarwal, and V. Aggarwal, "Joint optimization of concave scalarized multi-objective reinforcement learning with policy gradient based algorithm," *Journal of Artificial Intelligence Research*, vol. 74, pp. 1565–1597, 2022.
- [118] K. Van Moffaert and A. Nowé, "Multi-objective reinforcement learning using sets of Pareto dominating policies," *Journal of Machine Learning Research*, vol. 15, no. 1, pp. 3483–3512, 2014.
- [119] K. Van Moffaert, M. M. Drugan, and A. Nowé, "Hypervolume-based multi-objective reinforcement learning," in *EMO*, 2013.
- [120] H. Wang, "Multi-objective reinforcement learning based on non-linear scalarization and long-short-term optimization," *Robotic Intelligence and Automation*, 2024.
- [121] M. Pirotta, S. Parisi, and M. Restelli, "Multi-objective reinforcement learning with continuous Pareto frontier approximation," in *AAAI*, 2015.

- [122] X. Lin, Z. Yang, and Q. Zhang, "Pareto set learning for neural multi-objective combinatorial optimization," in *ICLR*, 2022.
- [123] T. Basaklar, S. Gumussoy, and U. Y. Ogras, "PD-MORL: Preference-driven multi-objective reinforcement learning algorithm," in *ICLR*, 2023.
- [124] B. Zhu, M. Dang, and A. Grover, "Scaling Pareto-efficient decision making via offline multi-objective RL," in *ICLR*, 2023.
- [125] T. Shu, K. Shang, C. Gong, Y. Nan, and H. Ishibuchi, "Learning Pareto set for multi-objective continuous robot control," in *IJCAI*, 2024.
- [126] E. Liu, Y.-C. Wu, X. Huang, C. Gao, R.-J. Wang, K. Xue, and C. Qian, "Pareto set learning for multi-objective reinforcement learning," in *AAAI*, 2025.
- [127] B. Shahriari, K. Swersky, Z. Wang, R. P. Adams, and N. De Freitas, "Taking the human out of the loop: A review of bayesian optimization," *Proceedings of the IEEE*, vol. 104, no. 1, pp. 148–175, 2015.
- [128] J. Knowles, "Parego: A hybrid algorithm with on-line landscape approximation for expensive multiobjective optimization problems," *IEEE Transactions on Evolutionary Computation*, vol. 10, no. 1, pp. 50–66, 2006.
- [129] Q. Zhang, W. Liu, E. Tsang, and B. Virginas, "Expensive multiobjective optimization by moea/d with gaussian process model," *IEEE Transactions on Evolutionary Computation*, vol. 14, no. 3, pp. 456–474, 2009.
- [130] R. Zhang and D. Golovin, "Random hypervolume scalarizations for provable multi-objective black box optimization," in *ICML*, 2020.
- [131] W. Ponweiser, T. Wagner, D. Biermann, and M. Vincze, "Multi-objective optimization on a limited budget of evaluations using model-assisted-metric selection," in *PPSN*, 2008.
- [132] M. Zuluaga, G. Sergent, A. Krause, and M. Püschel, "Active learning for multi-objective optimization," in *ICML*, 2013.
- [133] M. Zuluaga, A. Krause *et al.*, "e-PAL: An active learning approach to the multi-objective optimization problem," *Journal of Machine Learning Research*, vol. 17, no. 104, pp. 1–32, 2016.
- [134] B. Paria, K. Kandasamy, and B. Póczos, "A flexible framework for multi-objective bayesian optimization using random scalarizations," in *UAI*, 2020.
- [135] D. R. Jones, M. Schonlau, and W. J. Welch, "Efficient global optimization of expensive black-box functions," *Journal of Global Optimization*, vol. 13, pp. 455–492, 1998.
- [136] M. T. Emmerich, K. C. Giannakoglou, and B. Naujoks, "Single- and multiobjective evolutionary optimization assisted by gaussian random field metamodelling," *IEEE Transactions on Evolutionary Computation*, vol. 10, no. 4, pp. 421–439, 2006.
- [137] K. Yang, M. Emmerich, A. Deutz, and T. Bäck, "Efficient computation of expected hypervolume improvement using box decomposition algorithms," *Journal of Global Optimization*, vol. 75, pp. 3–34, 2019.
- [138] S. Daulton, M. Balandat, and E. Bakshy, "Differentiable expected hypervolume improvement for parallel multi-objective bayesian optimization," in *NeurIPS*, 2020.
- [139] K. Yang, M. Emmerich, A. Deutz, and T. Bäck, "Multi-objective bayesian global optimization using expected hypervolume improvement gradient," *Swarm and Evolutionary Computation*, vol. 44, pp. 945–956, 2019.
- [140] M. Konakovic Lukovic, Y. Tian, and W. Matusik, "Diversity-guided multi-objective bayesian optimization with batch evaluations," in *NeurIPS*, 2020.
- [141] S. Daulton, M. Balandat, and E. Bakshy, "Parallel bayesian optimization of multiple noisy objectives with expected hypervolume improvement," in *NeurIPS*, 2021.
- [142] S. Daulton, D. Eriksson, M. Balandat, and E. Bakshy, "Multi-objective bayesian optimization over high-dimensional search spaces," in *UAI*, 2022.
- [143] S. Daulton, M. Balandat, and E. Bakshy, "Hypervolume knowledge gradient: a lookahead approach for multi-objective bayesian optimization with partial information," in *ICML*, 2023.
- [144] S. Ament, S. Daulton, D. Eriksson, M. Balandat, and E. Bakshy, "Unexpected improvements to expected improvement for bayesian optimization," in *NeurIPS*, 2023.
- [145] D. Hernández-Lobato, J. Hernandez-Lobato, A. Shah, and R. Adams, "Predictive entropy search for multi-objective bayesian optimization," in *ICML*, 2016.
- [146] S. Belakaria, A. Deshwal, and J. R. Doppa, "Max-value entropy search for multi-objective bayesian optimization," in *NeurIPS*, 2019.
- [147] S. Suzuki, S. Takeno, T. Tamura, K. Shitara, and M. Karasuyama, "Multi-objective bayesian optimization using Pareto-frontier entropy," in *ICML*, 2020.
- [148] B. Tu, A. Gandy, N. Kantas, and B. Shafei, "Joint entropy search for multi-objective bayesian optimization," in *NeurIPS*, 2022.
- [149] C. Hvarfner, F. Hutter, and L. Nardi, "Joint entropy search for maximally-informed bayesian optimization," in *NeurIPS*, 2022.
- [150] S. Belakaria, A. Deshwal, N. K. Jayakodi, and J. R. Doppa, "Uncertainty-aware search framework for multi-objective bayesian optimization," in *AAAI*, 2020.
- [151] X. Lin, Z. Yang, X. Zhang, and Q. Zhang, "Pareto set learning for expensive multi-objective optimization," in *NeurIPS*, 2022.
- [152] B. Li, Z. Di, Y. Lu, H. Qian, F. Wang, P. Yang, K. Tang, and A. Zhou, "Expensive multi-objective bayesian optimization based on diffusion models," *arXiv preprint arXiv:2405.08674*, 2024.
- [153] M.-D. Nguyen, P. M. Dinh, Q.-H. Nguyen, L. P. Hoang, and D. D. Le, "Improving Pareto set learning for expensive multi-objective optimization via stein variational hypernetworks," in *AAAI*, 2024.
- [154] Y. Lu, B. Li, and A. Zhou, "Are you concerned about limited function evaluations: Data-augmented Pareto set learning for expensive multi-objective optimization," in *AAAI*, 2024.
- [155] K. Ishihara, A. Kanervisto, J. Miura, and V. Hautamaki, "Multi-task learning with attention for end-to-end autonomous driving," in *CVPR*, 2021.
- [156] X. Liang, X. Liang, and H. Xu, "Multi-task perception for autonomous driving," in *Autonomous Driving Perception: Fundamentals and Applications*, 2023.
- [157] X. Xu, H. Zhao, V. Vineet, S.-N. Lim, and A. Torralba, "MTFormer: Multi-task learning via transformer and cross-task reasoning," in *ECCV*, 2022.
- [158] H. Ye and D. Xu, "Inverted pyramid multi-task transformer for dense scene understanding," in *ECCV*, 2022.
- [159] B. Lin, W. Jiang, P. Chen, Y. Zhang, S. Liu, and Y.-C. Chen, "MTMamba: Enhancing multi-task dense scene understanding by mamba-based decoders," in *ECCV*, 2024.
- [160] B. Lin, W. Jiang, P. Chen, S. Liu, and Y.-C. Chen, "MTMamba++: Enhancing multi-task dense scene understanding via mamba-based decoders," *arXiv preprint arXiv:2408.15101*, 2024.
- [161] W.-H. Li, X. Liu, and H. Bilen, "Universal representations: A unified look at multiple task and domain learning," *International Journal of Computer Vision*, vol. 132, no. 5, pp. 1521–1545, 2024.
- [162] T. Xie, S. Wang, K. Wang, L. Yang, Z. Jiang, X. Zhang, K. Dai, R. Li, and J. Cheng, "Poly-PC: A polyhedral network for multiple point cloud tasks at once," in *CVPR*, 2023.
- [163] T. Xie, K. Dai, Q. Sun, Z. Jiang, C. Cao, L. Zhao, K. Wang, and R. Li, "CO-Net++: A cohesive network for multiple point cloud tasks at once with two-stage feature rectification," *IEEE Transactions on Pattern Analysis and Machine Intelligence*, 2024.
- [164] Z. Wang, Y. Li, H. Zhao, and S. Wang, "One for all: Multi-domain joint training for point cloud based 3d object detection," in *NeurIPS*, 2024.
- [165] S. Kyung, J. Won, S. Pak, S. Kim, S. Lee, K. Park, G.-S. Hong, and N. Kim, "Generative adversarial network with robust discriminator through multi-task learning for low-dose ct denoising," *IEEE Transactions on Medical Imaging*, 2024.
- [166] D. Ye, Y. Xie, W. Chen, Z. Zhou, L. Ge, and H. Foroosh, "LPFormer: Lidar pose estimation transformer with multi-task network," in *ICRA*, 2024.
- [167] P. Ren, Y. Xiao, X. Chang, P.-Y. Huang, Z. Li, X. Chen, and X. Wang, "A comprehensive survey of neural architecture search: Challenges and solutions," *ACM Computing Surveys*, vol. 54, no. 4, pp. 1–34, 2021.
- [168] H. Liu, K. Simonyan, and Y. Yang, "DARTS: differentiable architecture search," in *ICLR*, 2019.
- [169] H. Cai, L. Zhu, and S. Han, "ProxylessNAS: Direct neural architecture search on target task and hardware," in *ICLR*, 2019.
- [170] Y. Wu, Z. Huang, S. Kumar, R. S. Sukthankar, R. Timofte, and L. Van Gool, "Trilevel neural architecture search for efficient single image super-resolution," *arXiv preprint arXiv:2101.06658*, 2021.
- [171] D. Wang, M. Li, C. Gong, and V. Chandra, "AttentiveNAS: Improving neural architecture search via attentive sampling," in *CVPR*, 2021.

- [172] Z. Yue, B. Lin, Y. Zhang, and C. Liang, "Effective, efficient and robust neural architecture search," in *IJCNN*, 2022.
- [173] R. S. Sukthanker, A. Zela, B. Staffler, S. Dooley, J. Grabocka, and F. Hutter, "Multi-objective differentiable neural architecture search," in *ICLR*, 2025.
- [174] Y. Zheng and D. X. Wang, "A survey of recommender systems with multi-objective optimization," *Neurocomputing*, vol. 474, pp. 141–153, 2022.
- [175] T. Di Noia, J. Rosati, P. Tomeo, and E. Di Sciascio, "Adaptive multi-attribute diversity for recommender systems," *Information Sciences*, vol. 382, pp. 234–253, 2017.
- [176] S. Patil, D. Banerjee, and S. Sural, "A graph theoretic approach for multi-objective budget constrained capsule wardrobe recommendation," *ACM Transactions on Information Systems*, vol. 40, no. 1, pp. 1–33, 2021.
- [177] A. Lacerda, "Multi-objective ranked bandits for recommender systems," *Neurocomputing*, vol. 246, pp. 12–24, 2017.
- [178] N. Milojkovic, D. Antognini, G. Bergamin, B. Faltings, and C. Musat, "Multi-gradient descent for multi-objective recommender systems," *arXiv preprint arXiv:2001.00846*, 2019.
- [179] X. Lin, H. Chen, C. Pei, F. Sun, X. Xiao, H. Sun, Y. Zhang, W. Ou, and P. Jiang, "A Pareto-efficient algorithm for multiple objective optimization in e-commerce recommendation," in *RecSys*, 2019.
- [180] B. Mitrevski, M. Filipovic, D. Antognini, E. L. Glaude, B. Faltings, and C. Musat, "Momentum-based gradient methods in multi-objective recommendation," *arXiv preprint arXiv:2009.04695*, 2020.
- [181] L. Yang, Z. Liu, J. Zhang, R. Murthy, S. Heinecke, H. Wang, C. Xiong, and P. S. Yu, "Personalized multi-task training for recommender system," *arXiv preprint arXiv:2407.21364*, 2024.
- [182] R. Xie, Y. Liu, S. Zhang, R. Wang, F. Xia, and L. Lin, "Personalized approximate Pareto-efficient recommendation," in *WWW*, 2021.
- [183] Y. Ge, X. Zhao, L. Yu, S. Paul, D. Hu, C.-C. Hsieh, and Y. Zhang, "Toward Pareto efficient fairness-utility trade-off in recommendation through reinforcement learning," in *WSDM*, 2022.
- [184] T. Wilm, P. Normann, and F. Stepprath, "Pareto front approximation for multi-objective session-based recommender systems," in *RecSys*, 2024.
- [185] B. Liu, C. Chen, Z. Gong, C. Liao, H. Wang, Z. Lei, M. Liang, D. Chen, M. Shen, H. Zhou, W. Jiang, H. Yu, and J. Li, "MFT-Coder: Boosting code LLMs with multitask fine-tuning," in *KDD*, 2024.
- [186] Z. Gong, H. Yu, C. Liao, B. Liu, C. Chen, and J. Li, "CoBa: Convergence balancer for multitask finetuning of large language models," in *EMNLP*, 2024.
- [187] Z. Wu, Y. Hu, W. Shi, N. Dziri, A. Suhr, P. Ammanabrolu, N. A. Smith, M. Ostendorf, and H. Hajishirzi, "Fine-grained human feedback gives better rewards for language model training," in *NeurIPS*, 2023.
- [188] Z. Zhou, J. Liu, J. Shao, X. Yue, C. Yang, W. Ouyang, and Y. Qiao, "Beyond one-preference-fits-all alignment: Multi-objective direct preference optimization," in *Findings of ACL*, 2024.
- [189] A. Rame, G. Couairon, C. Dancette, J.-B. Gaya, M. Shukor, L. Soulier, and M. Cord, "Rewarded soups: towards Pareto-optimal alignment by interpolating weights fine-tuned on diverse rewards," in *NeurIPS*, 2023.
- [190] J. Jang, S. Kim, B. Y. Lin, Y. Wang, J. Hessel, L. Zettlemoyer, H. Hajishirzi, Y. Choi, and P. Ammanabrolu, "Personalized soups: Personalized large language model alignment via post-hoc parameter merging," *arXiv preprint arXiv:2310.11564*, 2023.
- [191] R. Shi, Y. Chen, Y. Hu, A. Liu, H. Hajishirzi, N. A. Smith, and S. S. Du, "Decoding-time language model alignment with multiple objectives," in *NeurIPS*, 2024.
- [192] H. Wang, Y. Lin, W. Xiong, R. Yang, S. Diao, S. Qiu, H. Zhao, and T. Zhang, "Arithmetic control of LLMs for diverse user preferences: Directional preference alignment with multi-objective rewards," in *ACL*, 2024.
- [193] Y. Guo, G. Cui, L. Yuan, N. Ding, Z. Sun, B. Sun, H. Chen, R. Xie, J. Zhou, Y. Lin *et al.*, "Controllable preference optimization: Toward controllable multi-objective alignment," in *EMNLP*, 2024.
- [194] R. Yang, X. Pan, F. Luo, S. Qiu, H. Zhong, D. Yu, and J. Chen, "Rewards-in-context: Multi-objective alignment of foundation models with dynamic preference adjustment," in *ICML*, 2024.
- [195] R. Yu, W. Chen, X. Wang, and J. Kwok, "Enhancing meta learning via multi-objective soft improvement functions," in *ICLR*, 2023.
- [196] H. Wang, H. Zhao, and B. Li, "Bridging multi-task learning and meta-learning: Towards efficient training and effective adaptation," in *ICML*, 2021.
- [197] Z. Hu, K. Shaloudegi, G. Zhang, and Y. Yu, "Federated learning meets multi-objective optimization," *IEEE Transactions on Network Science and Engineering*, vol. 9, no. 4, pp. 2039–2051, 2022.
- [198] B. Askin, P. Sharma, G. Joshi, and C. Joe-Wong, "Federated communication-efficient multi-objective optimization," *arXiv preprint arXiv:2410.16398*, 2024.
- [199] Y. Kang, H. Gu, X. Tang, Y. He, Y. Zhang, J. He, Y. Han, L. Fan, K. Chen, and Q. Yang, "Optimizing privacy, utility, and efficiency in a constrained multi-objective federated learning framework," *ACM Transactions on Intelligent Systems and Technology*, vol. 15, no. 6, 2024.
- [200] W. Li, F. Lyu, F. Shang, L. Wan, and W. Feng, "Long-tailed learning as multi-objective optimization," in *AAAI*, 2024.
- [201] Z. Zhao, P. Wang, H. Wen, W. Xu, S. Lai, Q. Zhang, and Y. Wang, "Two fists, one heart: Multi-objective optimization based strategy fusion for long-tailed learning," in *ICML*, 2024.
- [202] Z. Zhou, L. Liu, P. Zhao, and W. Gong, "Pareto deep long-tailed recognition: A conflict-averse solution," in *ICLR*, 2024.
- [203] S. Lai, Z. Zhao, F. Zhu, X. Lin, Q. Zhang, and G. Meng, "Pareto continual learning: Preference-conditioned learning and adaptation for dynamic stability-plasticity trade-off," in *AAAI*, 2025.
- [204] T. Hang, S. Gu, C. Li, J. Bao, D. Chen, H. Hu, X. Geng, and B. Guo, "Efficient diffusion training via min-snr weighting strategy," in *ICCV*, 2023.
- [205] H. Go, Y. Lee, S. Lee, S. Oh, H. Moon, and S. Choi, "Addressing negative transfer in diffusion models," in *NeurIPS*, 2023.
- [206] Z. Xu, Y. Chen, H.-a. Gao, W. Zhao, G. Zhang, and H. Zhao, "Diffusion-based visual anagram as multi-task learning," in *WACV*, 2025.
- [207] Y. Yao, Y. Pan, J. Li, I. Tsang, and X. Yao, "PROUD: PaRetO-gUided diffusion model for multi-objective generation," *Machine Learning*, vol. 113, no. 9, pp. 6511–6538, 2024.
- [208] K. Li, T. Zhang, and R. Wang, "Deep reinforcement learning for multiobjective optimization," *IEEE Transactions on Cybernetics*, vol. 51, no. 6, pp. 3103–3114, 2020.
- [209] Z. Wang, S. Yao, G. Li, and Q. Zhang, "Multiobjective combinatorial optimization using a single deep reinforcement learning model," *IEEE Transactions on Cybernetics*, 2023.
- [210] J. Chen, Z. Zhang, Z. Cao, Y. Wu, Y. Ma, T. Ye, and J. Wang, "Neural multi-objective combinatorial optimization with diversity enhancement," in *NeurIPS*, 2023.
- [211] J. Chen, J. Wang, Z. Zhang, Z. Cao, T. Ye, and S. Chen, "Efficient meta neural heuristic for multi-objective combinatorial optimization," in *NeurIPS*, 2023.
- [212] M. Jain, S. C. Rappaport, A. Hernández-García, J. Rector-Brooks, Y. Bengio, S. Miret, and E. Bengio, "Multi-objective GFlowNets," in *ICML*, 2023.
- [213] Y. Zhu, J. Wu, C. Hu, J. Yan, T. Hou, and J. Wu, "Sample-efficient multi-objective molecular optimization with GFlowNets," in *NeurIPS*, 2023.
- [214] Y. Hwang and D.-Y. Lim, "Dual cone gradient descent for training physics-informed neural networks," in *NeurIPS*, 2024.
- [215] Q. Liu, M. Chu, and N. Thurey, "ConFIG: Towards conflict-free training of physics informed neural networks," in *ICLR*, 2025.
- [216] B. Lin and Y. Zhang, "LibMTL: A Python library for deep multi-task learning," *Journal of Machine Learning Research*, vol. 24, no. 209, pp. 1–7, 2023.
- [217] X. Zhang, L. Zhao, Y. Yu, X. Lin, Y. Chen, H. Zhao, and Q. Zhang, "LibMOON: A gradient-based multiobjective optimization library in PyTorch," in *NeurIPS*, 2024.
- [218] A. Paszke, S. Gross, F. Massa, A. Lerer, J. Bradbury, G. Chanan, T. Killeen, Z. Lin, N. Gimselshein, L. Antiga, A. Desmaison, A. Köpf, E. Yang, Z. DeVito *et al.*, "PyTorch: An imperative style, high-performance deep learning library," in *NeurIPS*, 2019.
- [219] N. Silberman, D. Hoiem, P. Kohli, and R. Fergus, "Indoor segmentation and support inference from RGBD images," in *ECCV*, 2012.
- [220] A. R. Zamir, A. Sax, W. Shen, L. J. Guibas, J. Malik, and S. Savarese, "Taskonomy: Disentangling task transfer learning," in *CVPR*, 2018.
- [221] M. Cordts, M. Omran, S. Ramos, T. Rehfeld, M. Enzweiler, R. Benenson, U. Franke, S. Roth, and B. Schiele, "The cityscapes dataset for semantic urban scene understanding," in *CVPR*, 2016.
- [222] R. Ramakrishnan, P. O. Dral, M. Rupp, and O. A. Von Lilienfeld, "Quantum chemistry structures and properties of 134 kilo molecules," *Scientific Data*, vol. 1, no. 1, pp. 1–7, 2014.

- [223] K. Saenko, B. Kulis, M. Fritz, and T. Darrell, "Adapting visual category models to new domains," in *ECCV*, 2010.
- [224] H. Venkateswara, J. Eusebio, S. Chakraborty, and S. Panchanathan, "Deep hashing network for unsupervised domain adaptation," in *CVPR*, 2017.
- [225] Z. Liu, P. Luo, X. Wang, and X. Tang, "Deep learning face attributes in the wild," in *ICCV*, 2015.
- [226] A. Krizhevsky and G. Hinton, "Learning multiple layers of features from tiny images," *Technical Report*, 2009.
- [227] T. Yu, D. Quillen, Z. He, R. Julian, K. Hausman, C. Finn, and S. Levine, "Meta-world: A benchmark and evaluation for multi-task and meta reinforcement learning," in *CoRL*, 2020.
- [228] J. Hu, S. Ruder, A. Siddhant, G. Neubig, O. Firat, and M. Johnson, "XTREME: A massively multilingual multi-task benchmark for evaluating cross-lingual generalisation," in *ICML*, 2020.
- [229] J. Ji, D. Hong, B. Zhang, B. Chen, J. Dai, B. Zheng, T. Qiu, B. Li, and Y. Yang, "PKU-SafeRLHF: Towards multi-level safety alignment for LLMs with human preference," *arXiv preprint arXiv:2406.15513*, 2024.
- [230] G. Cui, L. Yuan, N. Ding, G. Yao, W. Zhu, Y. Ni, G. Xie, Z. Liu, and M. Sun, "Ultrafeedback: Boosting language models with high-quality feedback," *arXiv preprint arXiv:2310.01377*, 2023.
- [231] Z. Wang, Y. Dong, O. Delalleau, J. Zeng, G. Shen, D. Egert, J. J. Zhang, M. N. Sreedhar, and O. Kuchaiev, "Helpsteer2: Open-source dataset for training top-performing reward models," in *NeurIPS*, 2024.
- [232] X. Zhang, X. Lin, B. Xue, Y. Chen, and Q. Zhang, "Hypervolume maximization: A geometric view of Pareto set learning," in *NeurIPS*, 2023.

APPENDIX A ILLUSTRATION OF KEY CONCEPTS IN MOO

Figure 6 illustrates the Pareto concepts on the two-objective problem. The blue circles represent **Pareto optimal solutions** (defined in Definition 2), which indicates that no solution can improve one objective without worsening the other. The blue curve connecting the blue circles denotes the **Pareto front**, as defined in Definition 3. The yellow circles indicate **weak Pareto optimal solutions** since they can be improved in one objective without negatively impacting the other. For example, comparing θ_2 and θ_1 , θ_2 is a weak Pareto optimal solution since it can be improved in the second objective without affecting the first. The red circles represent solutions that are **not Pareto optimal** because there exists another solution that strictly Pareto dominates them. For instance, comparing θ_3 and θ_1 , θ_3 is not a Pareto optimal solution as θ_1 outperforms it in both objectives.

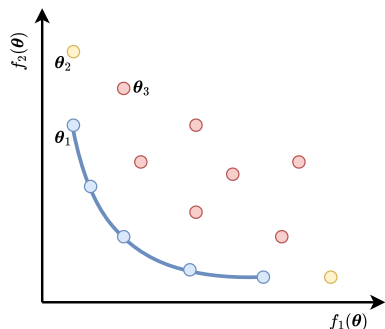


Fig. 6: Illustration of Pareto optimality concepts. The blue, yellow, and red circles denote Pareto optimal solutions, weakly Pareto optimal solutions, and dominated solutions, respectively. The blue curve represents the Pareto front.

APPENDIX B ADDITIONAL DETAILS AND FURTHER RESULTS FOR THE EXPERIMENT IN FIG. 4

To demonstrate the differences in the solution distributions produced by various methods, we consider a commonly used benchmark problem, LSMOP1 [84]. Each algorithm is run for 5000 iterations. The solutions obtained by PTML [36], EPO [37], [38], GradHV [47], and MOO-SVGD [48] are shown in Figure 4 in the main paper. Additionally, the solutions generated by MGDA [6], PMGDA [40], UMOD [43], and Smooth Tchebycheff [18] are shown in Figure 7.

From Figures 4 and 7, we can observe that MGDA, which does not incorporate preferences, exhibits poor diversity. The constraint-based approach in PTML produces solutions that are better aligned with the preference vector but still fall short of exact alignment. EPO and PMGDA achieves exact alignment with the preference vector. Some methods that do not use a preference vector, such as GradHV and MOO-SVGD, are also able to produce diverse solutions.

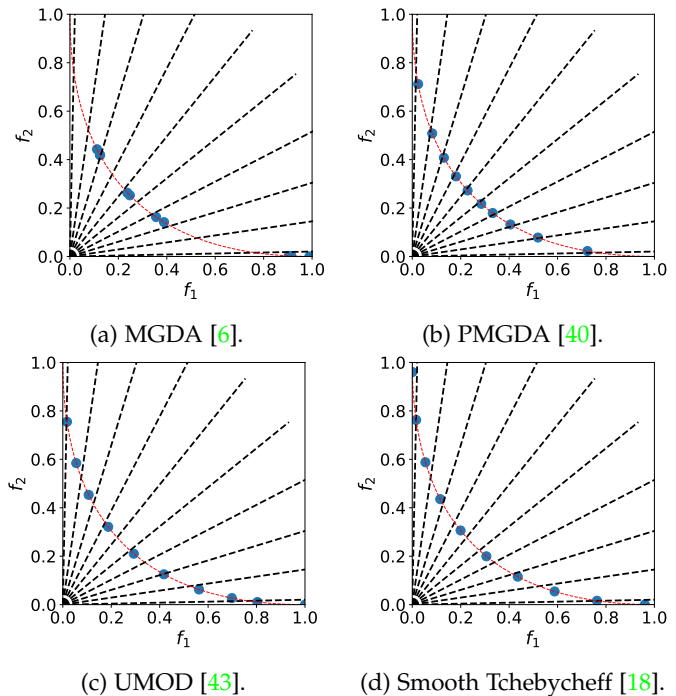


Fig. 7: Distributions of solutions obtained by using MGDA [6], PMGDA [40], UMOD [43], and Smooth Tchebycheff [18]. The blue circles denote the solutions, the red curves denote the ground truth PF and the black lines denote the preference vectors.

APPENDIX C DETAILS OF BENCHMARK DATASETS

In this section, we list the details of benchmark datasets in Section 8.

- **NYUv2** dataset [219] is for indoor scene understanding. It has three tasks (i.e., semantic segmentation, depth estimation, and surface normal prediction) with 795 training and 654 testing samples.
- **Taskonomy** dataset [220] is obtained from 3D scans of about 600 buildings and contains 26 tasks (such as semantic segmentation, depth estimation, surface normal prediction, keypoint detection, and edge detection) with about 4 million samples.
- **Cityscapes** dataset [221] is for urban scene understanding. It has two tasks (i.e., semantic segmentation and depth estimation) with 2,975 training and 500 testing samples.
- **QM9** dataset [222] is for molecular property prediction with 11 tasks. Each task performs regression on one property. It contains 130,000 samples.
- **Office-31** dataset [223] contains 4,110 images from three domains (tasks): Amazon, DSLR, and Webcam. Each task has 31 classes.
- **Office-Home** dataset [224] contains 15,500 images from four domains (tasks): artistic images, clipart, product images, and real-world images. Each task has 65 object categories collected under office and home settings.
- **CelebA** dataset [225] is a large-scale face attributes dataset, containing 202,599 face images. Each image has 40 attribute annotation. Hence, this dataset includes

40 tasks and each of them is a binary classification problem for one attribute.

- **CIFAR-100** dataset [226] an image classification with 100 classes, containing 50,000 training and 10,000 testing image samples. These 100 classes are divided into 20 tasks, each of which is a 5-class image classification problem.
- **MT10** and **MT50** from Meta-World benchmark [227] are two multi-task reinforcement learning settings, containing 10 and 50 robot manipulation tasks, respectively.
- **XTREME** benchmark [228] aims to evaluate the cross-lingual generalization abilities of multilingual representations. It contains 9 tasks in 40 languages, including 2 classification tasks, 2 structure prediction tasks, 3 question-answering tasks, and 2 sentence retrieval tasks.
- **PKU-SafeRLHF** dataset [229] focuses on safety alignment in LLMs, containing 82,118 question-answering pairs with the annotations of helpfulness and harmlessness.
- **UltraFeedBack** dataset [230] contains 63,967 prompts, each corresponding to four responses from different LLMs. Each response has 4 aspects of annotations, namely instruction-following, truthfulness, honesty, and helpfulness, generated by GPT-4.
- **HelpSteer2** dataset [231] contains 21,362 samples. Each sample contains a prompt and a response with 5 human-annotated attributes (i.e., helpfulness, correctness, coherence, complexity, and verbosity), each ranging between 0 and 4 where higher means better for each attribute.